

재료상변태

Phase Transformation of Materials

2008. 10. 16.

박 은 수

서울대학교 재료공학부

Contents for previous class

- Diffusion in multiphase binary system

Chapter 3 Crystal Interfaces and Microstructure

- Interfacial Free Energy

→ The Gibbs free energy of a system containing an interface of area A

$$\rightarrow G_{\text{bulk}} + G_{\text{interface}} \begin{array}{|c|} \hline \text{vapor} \\ \hline \text{solid} \\ \hline \end{array} \rightarrow G = G_0 + \gamma A$$

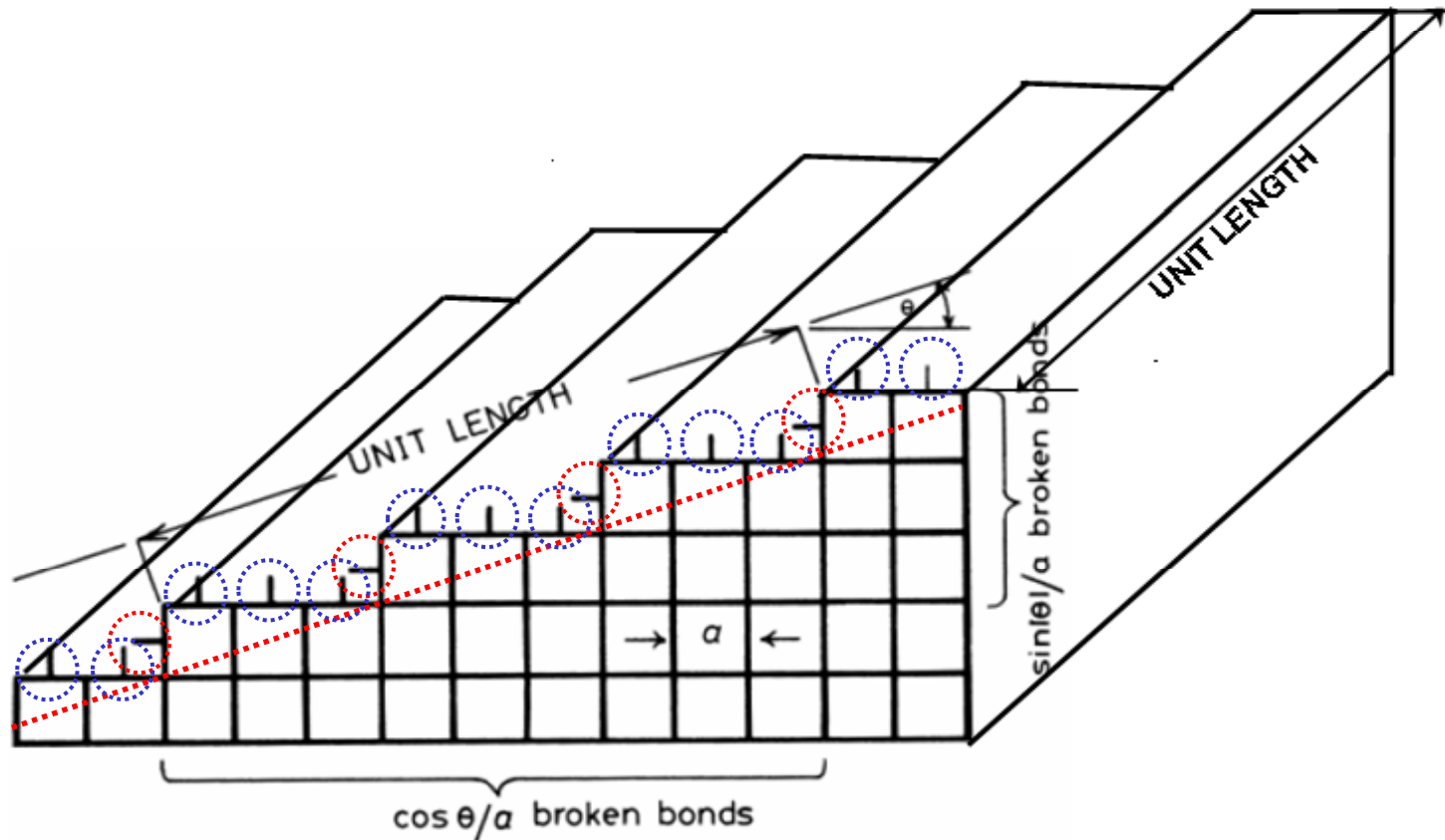
- Solid/Vapor Interfaces

Origin of the surface free energy? → Broken Bonds

Equilibrium shape → Wulff surface

Surface energy for high or irrational {hkl} index

A crystal plane at an angle θ to the close-packed plane will contain broken bonds in excess of the close-packed plane due to the atoms at the steps.



$(\cos\theta/a)(1/a)$: broken bonds from the atoms on the steps

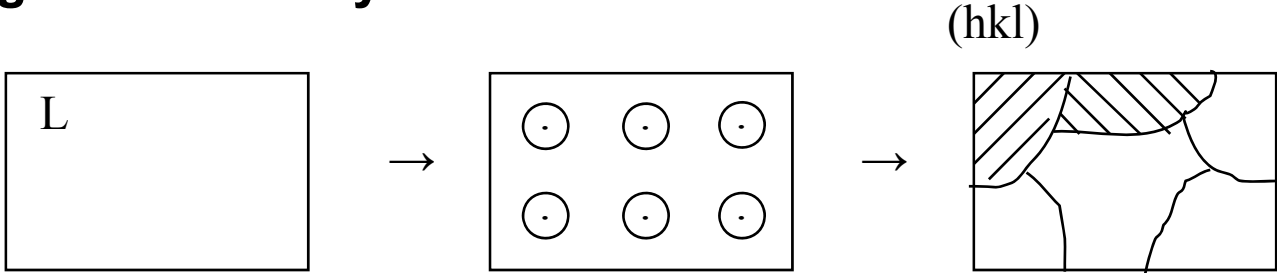
$(\sin|\theta|/a)(1/a)$: additional broken bonds from the atoms on the steps

Contents for today's class

- **Boundaries in Single-Phase Solids**
 - (a) **Low-Angle and High-Angle Boundaries**
 - (b) **Special High-Angle Grain Boundaries**
 - (c) **Equilibrium in Polycrystalline Materials**

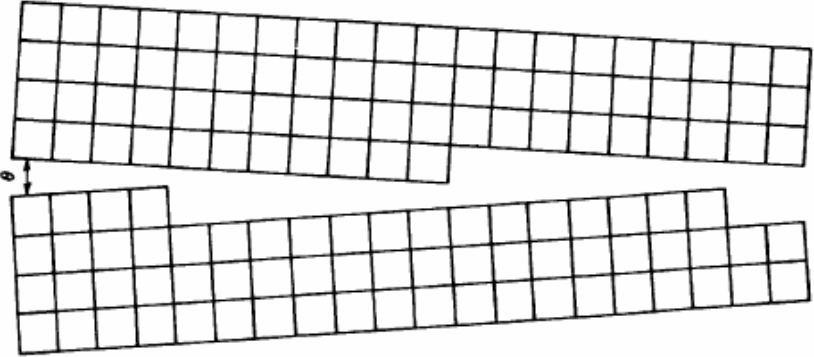
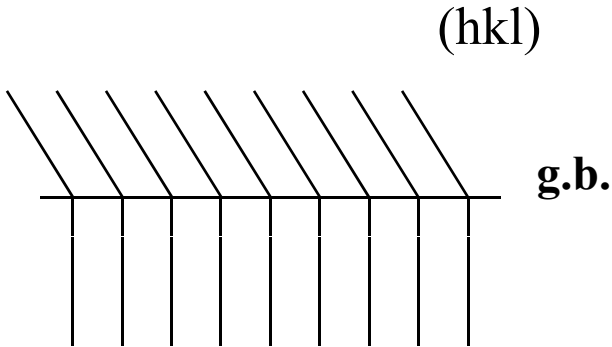
Boundaries in Single-Phase Solids

grain boundary

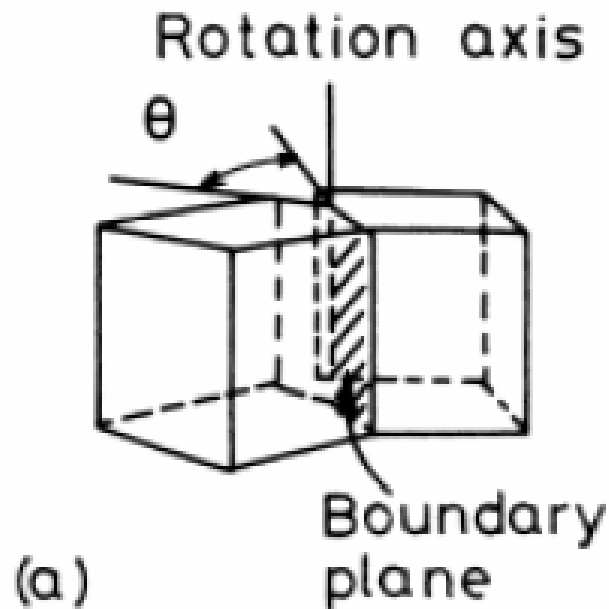


- 1) misorientation of lattice in two grains
- 2) orientation of grain boundary

Single phase
Poly grain

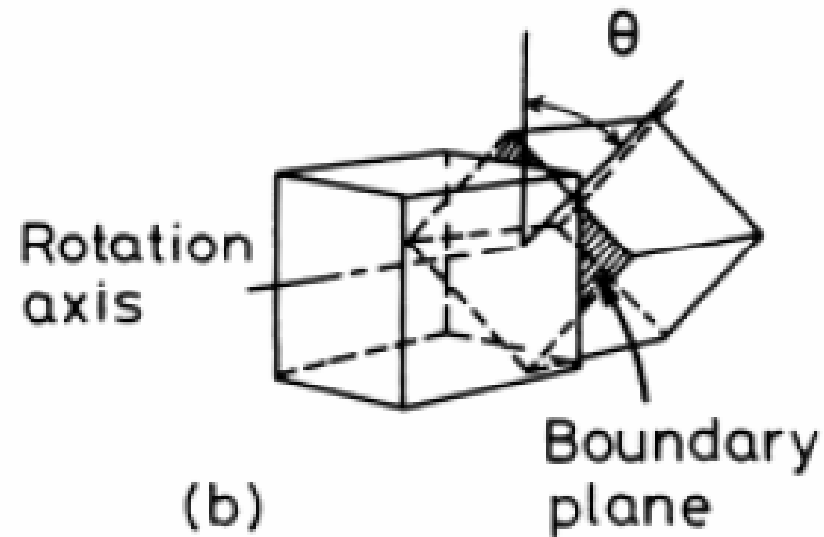


3.3 Boundaries in Single-Phase Solids



tilt boundary

$\theta \rightarrow$ misorientation
 \rightarrow tilt angle



twist boundary

$\theta \rightarrow$ misorientation
 \rightarrow twist angle

[symmetric tilt or twist boundary
[non-symmetric tilt or twist boundary

3.3.1 Low-Angle and High-Angle Boundaries

Low-Angle Boundaries

Symmetrical low-angle tilt boundary

Symmetrical low-angle twist boundary

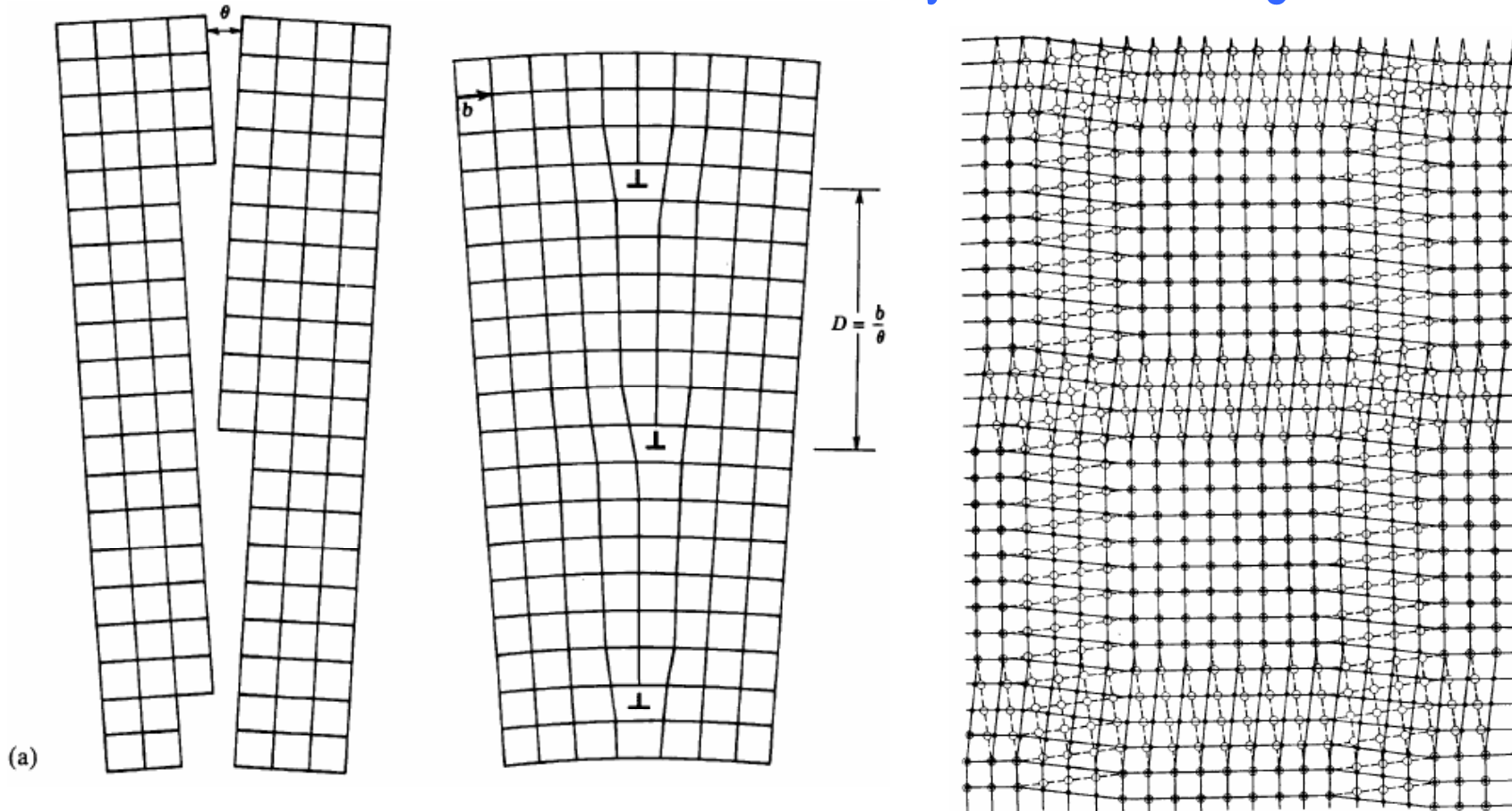


Fig. 3.7 (a) Low-angle tilt boundary, (b) low-angle twist boundary: \circ atoms in crystal below, \bullet atoms in crystal above boundary. (After W.T. Read Jr., *Dislocations in crystals*, McGraw-Hill, New York, 1953.)

Fig. 3.7 (b)

tilt Boundaries

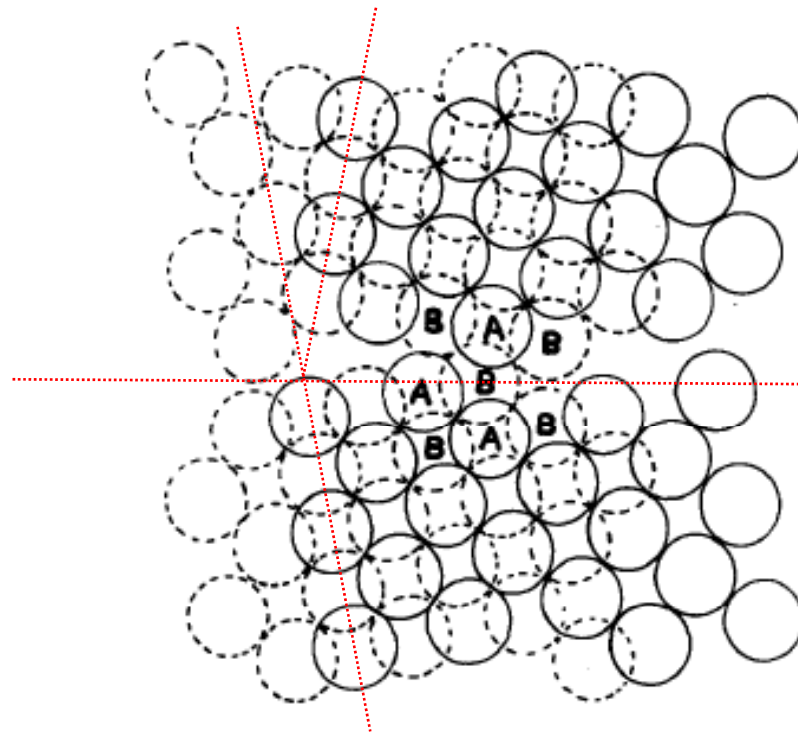
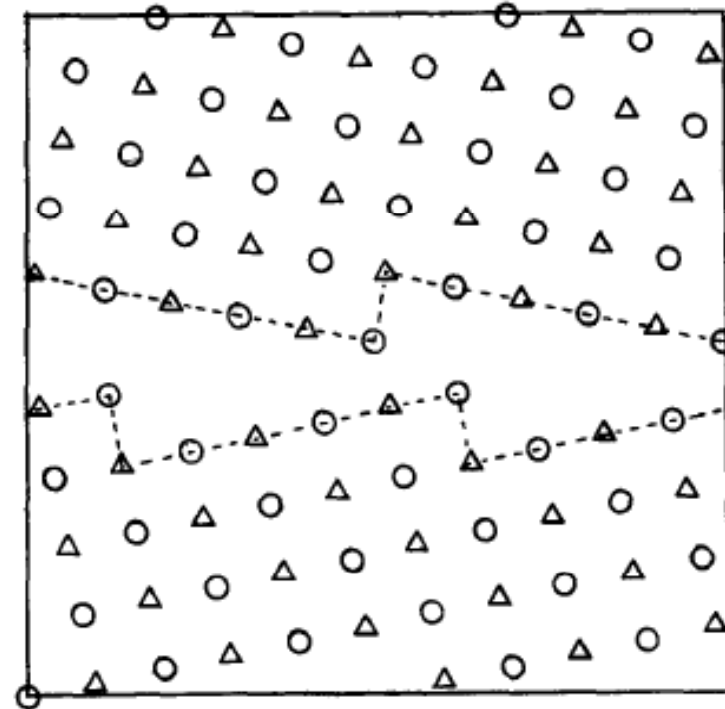
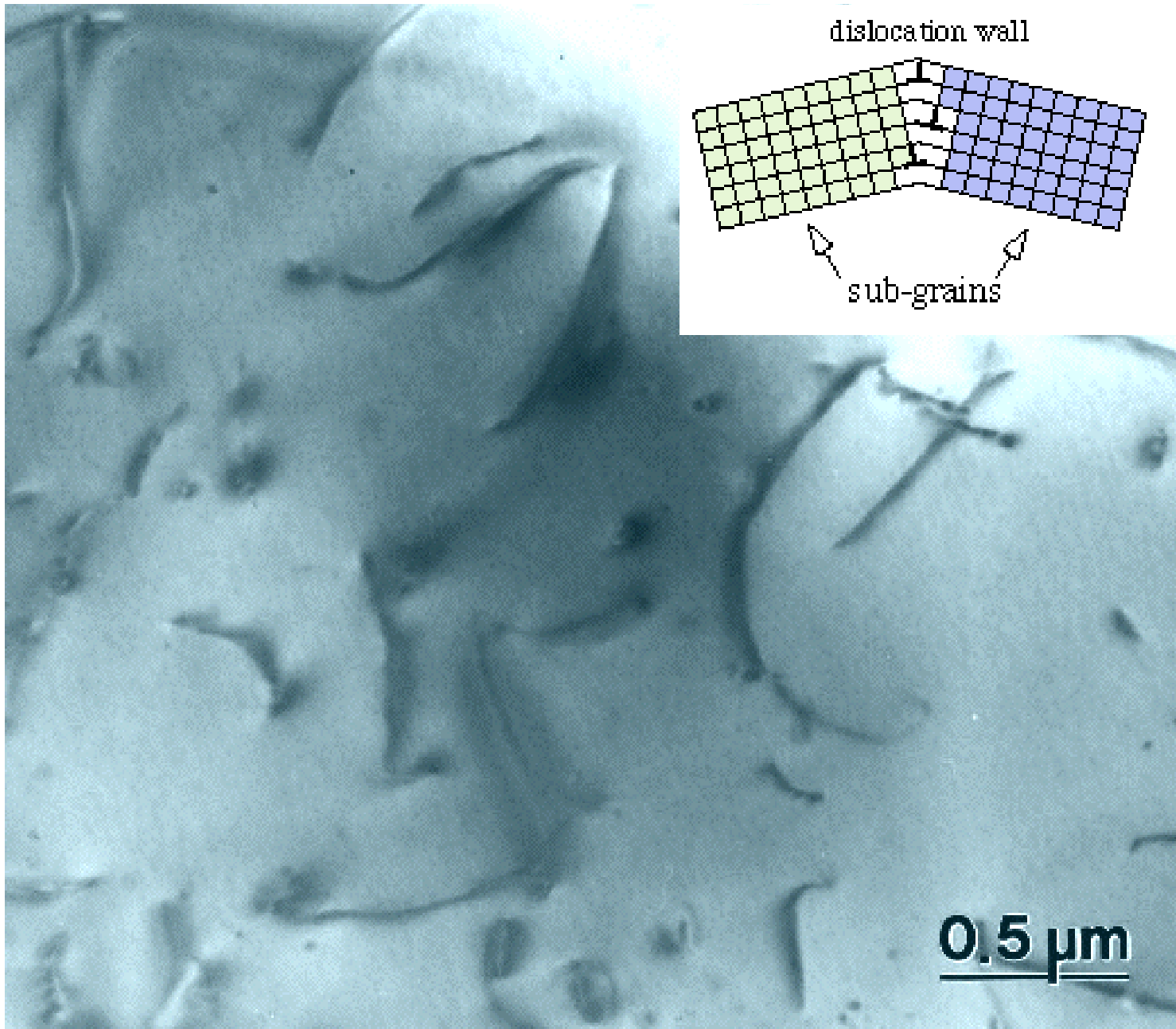


Figure 1 - 23° symmetric tilt boundary about a $\langle 001 \rangle$ axis. The circles with dashed lines represent one layer and the circles with solid lines the other layer of the AB...stacked $\{001\}$ planes. The atoms labelled A and B denote the structural unit.

Figure 2 - 23° symmetric tilt boundary about a $\langle 001 \rangle$ axis. Δ represent one layer and \circ represent the other layer of the AB..... stacked $\{001\}$ planes. The ledge like character of the boundary is shown by the dashed lines.



Dislocations



twist Boundaries

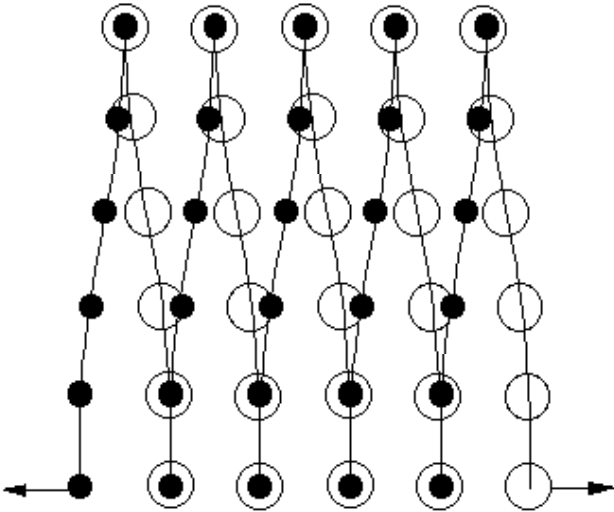
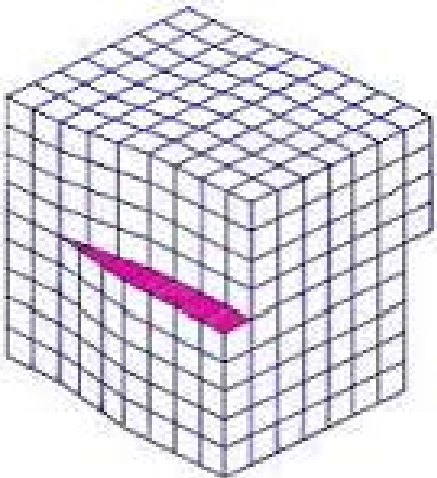
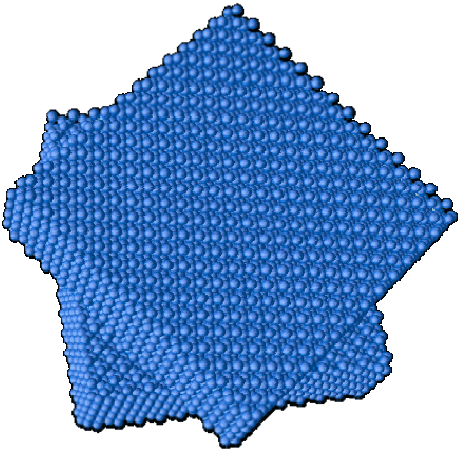
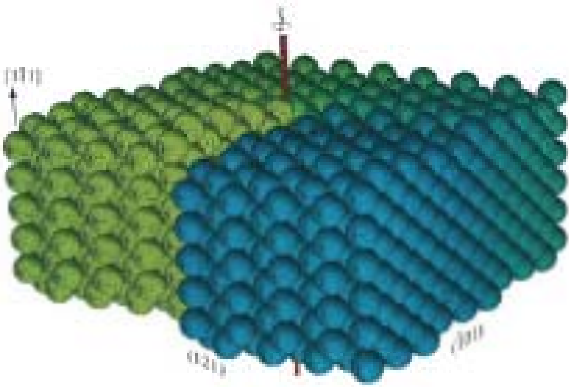
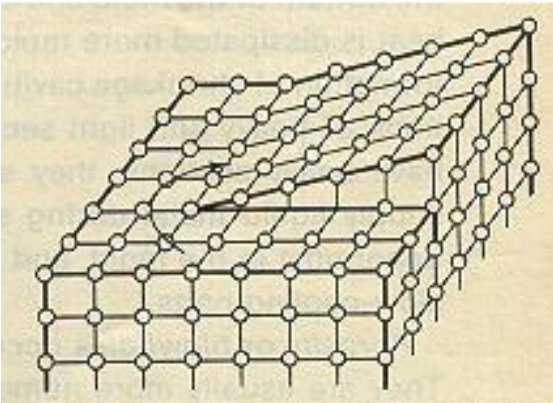
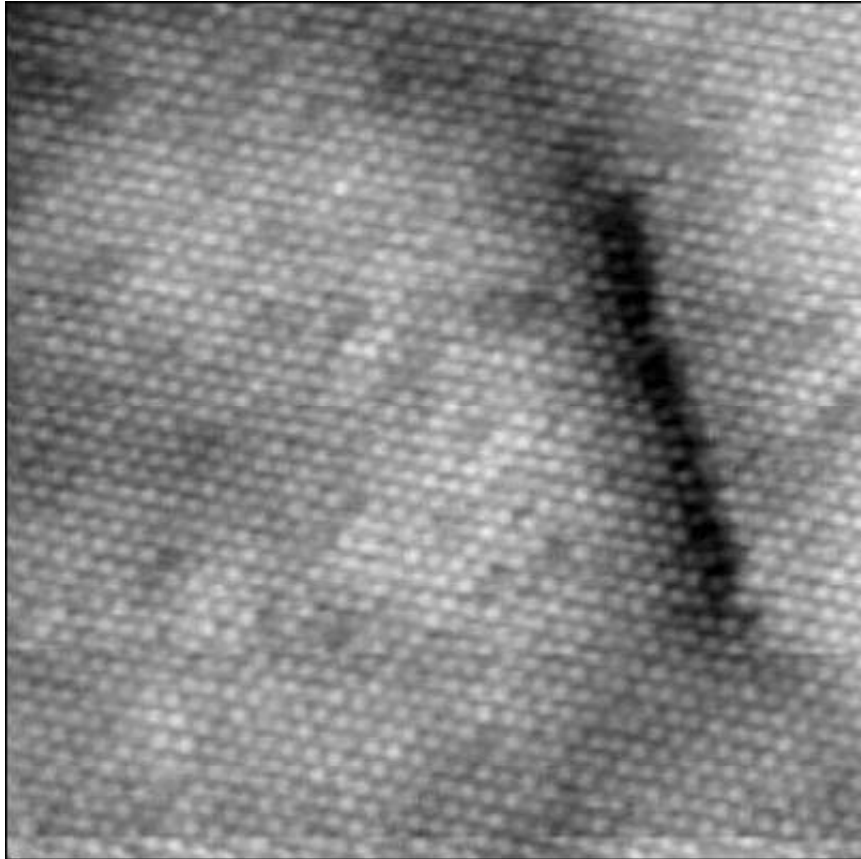


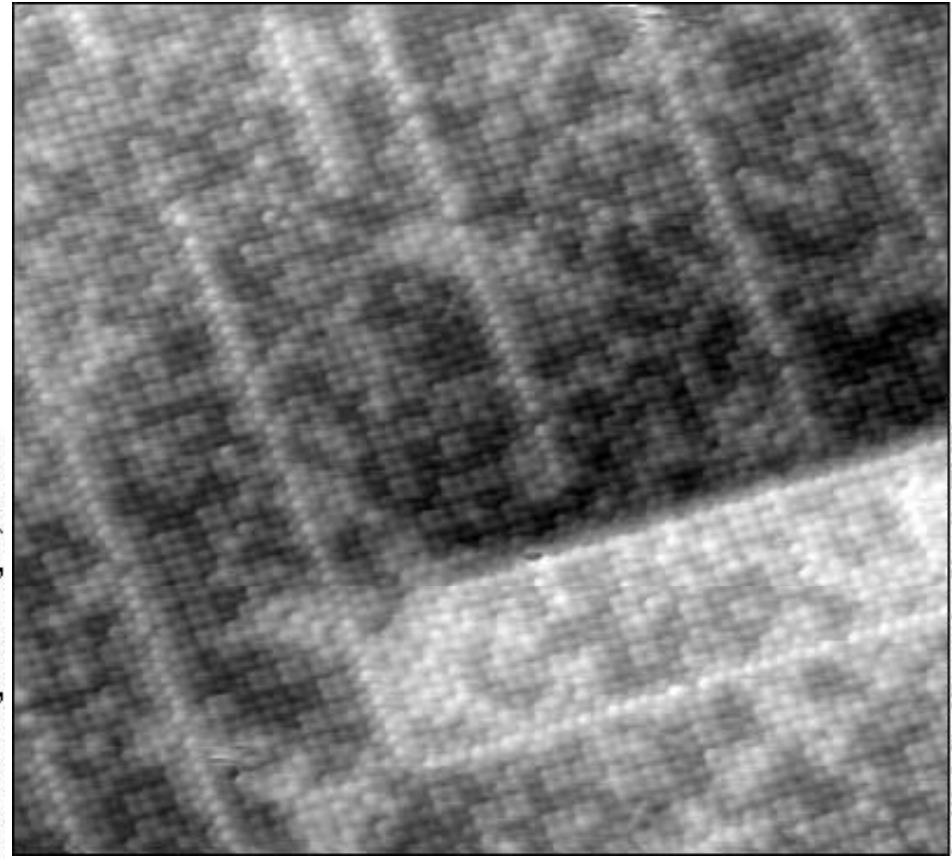
Figure 2. A screw dislocation; note the screw-like 'slip' of atoms in the upper part of the lattice



Screw dislocation

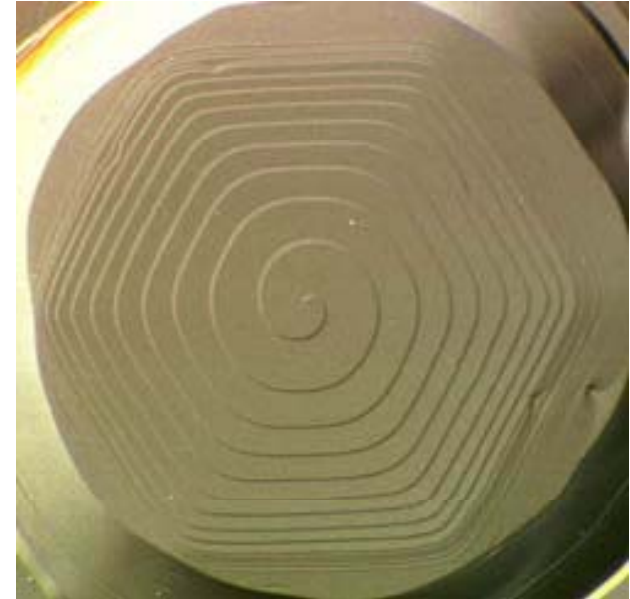
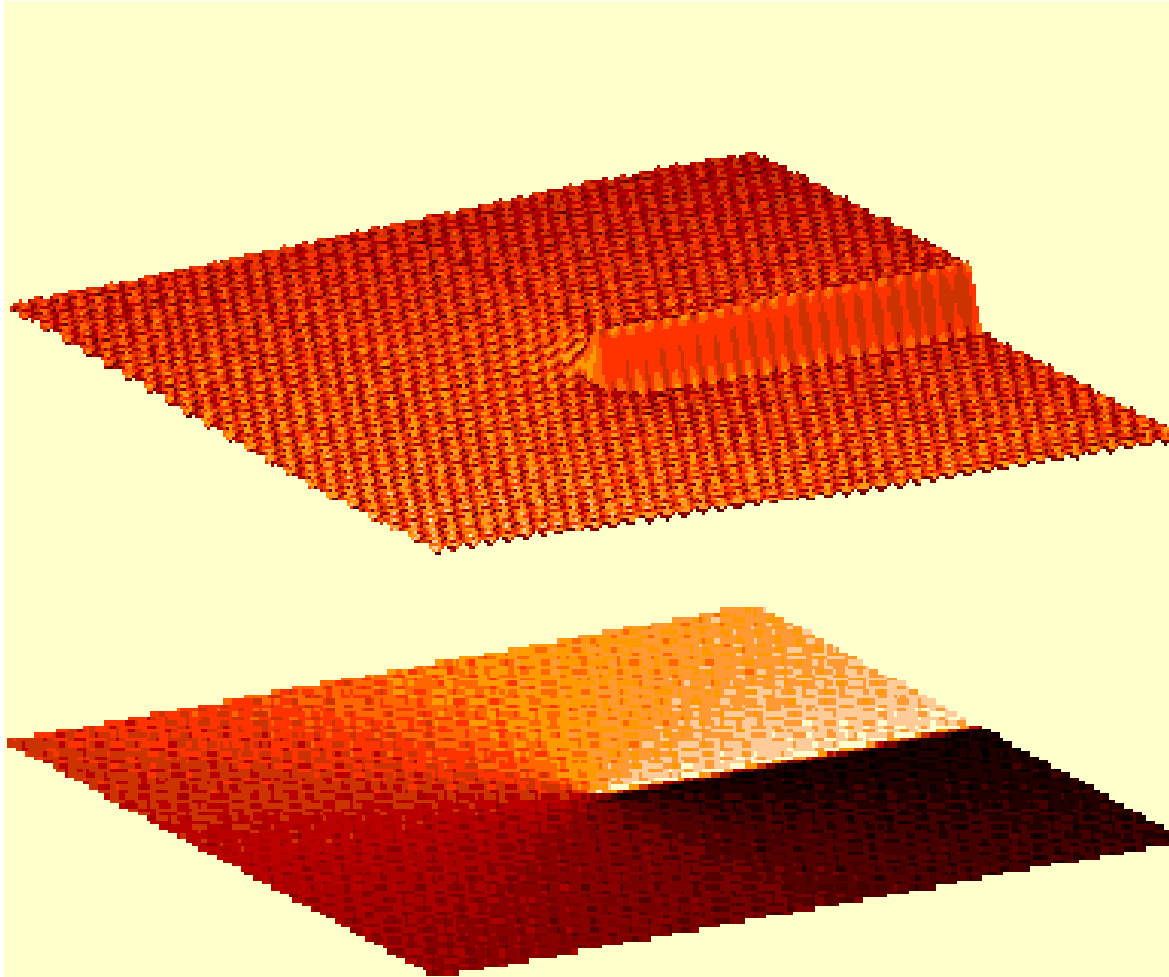


Institut für Allgemeine Physik, TU Wien

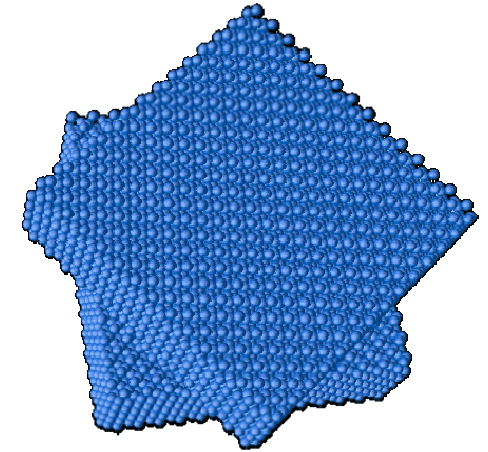
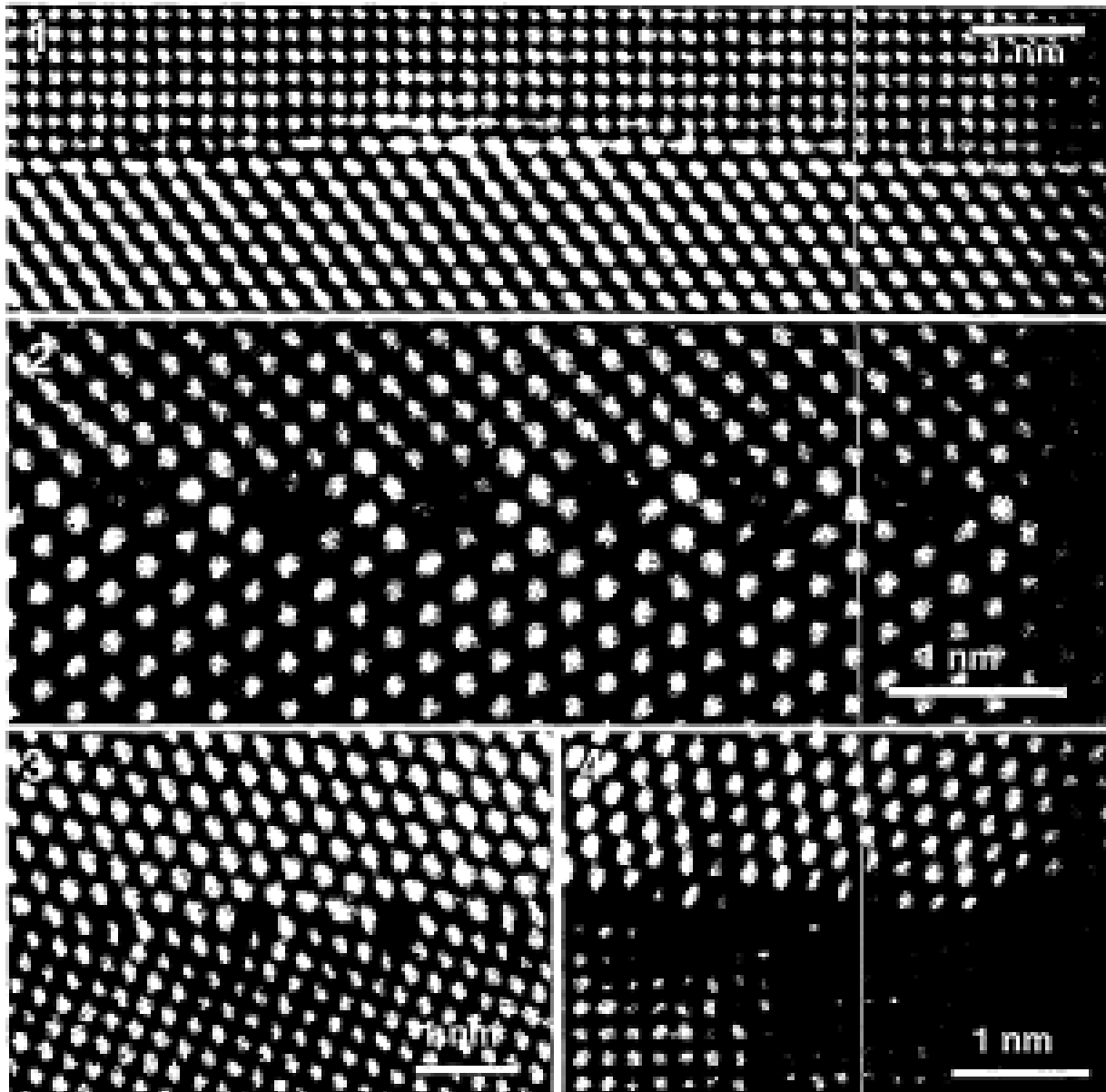


Institut für Allgemeine Physik, TU Wien

Growth of Screw dislocation



twist Boundaries



45°, (010) symmetric twist GB

90°, (110) symmetric twist GB

Asymmetric GB
with tilt and twist components

Non-symmetric Tilt Boundary

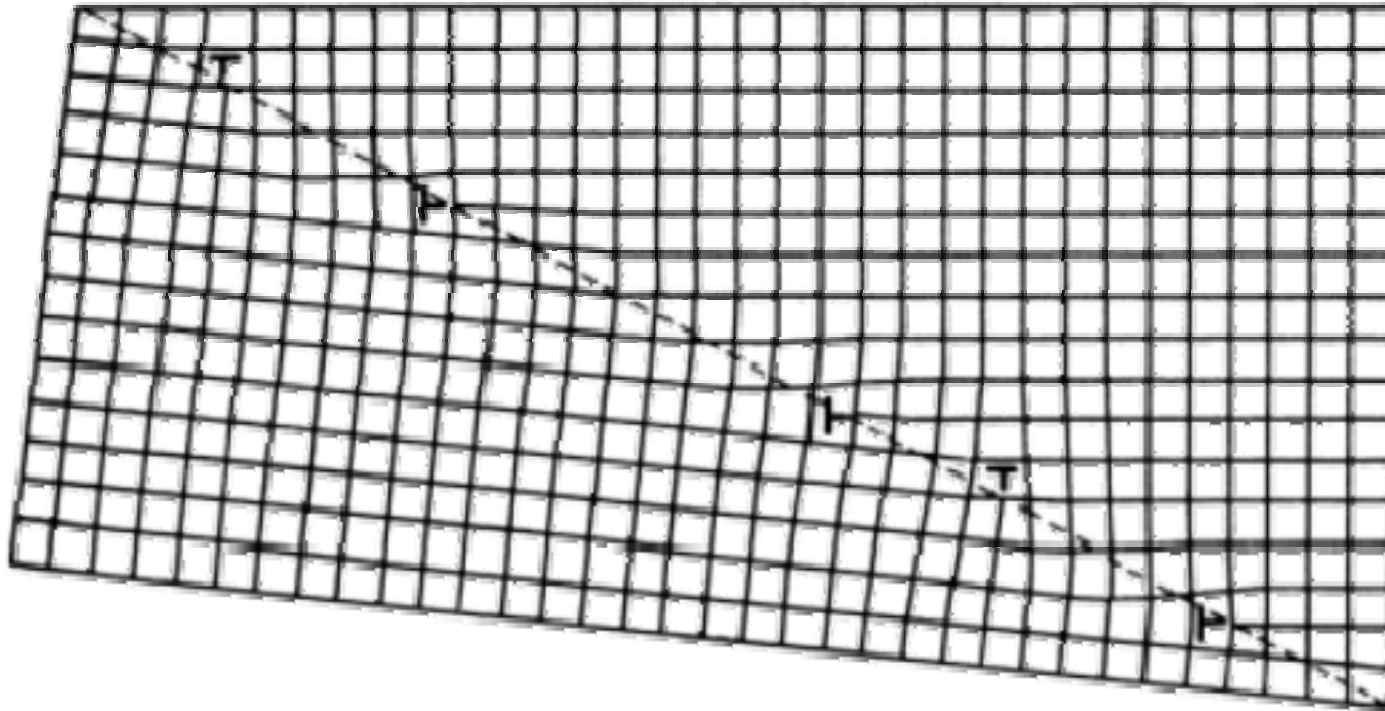


Fig. 3.8 An unsymmetric tilt boundary. Dislocations with two different Burgers vectors are present. (After W.T. Read Jr., *Dislocations in Crystals*, McGraw-Hill, New York, 1953.)

If the boundary is unsymmetrical, dislocations with different Burgers vectors are required to accommodate the misfit.

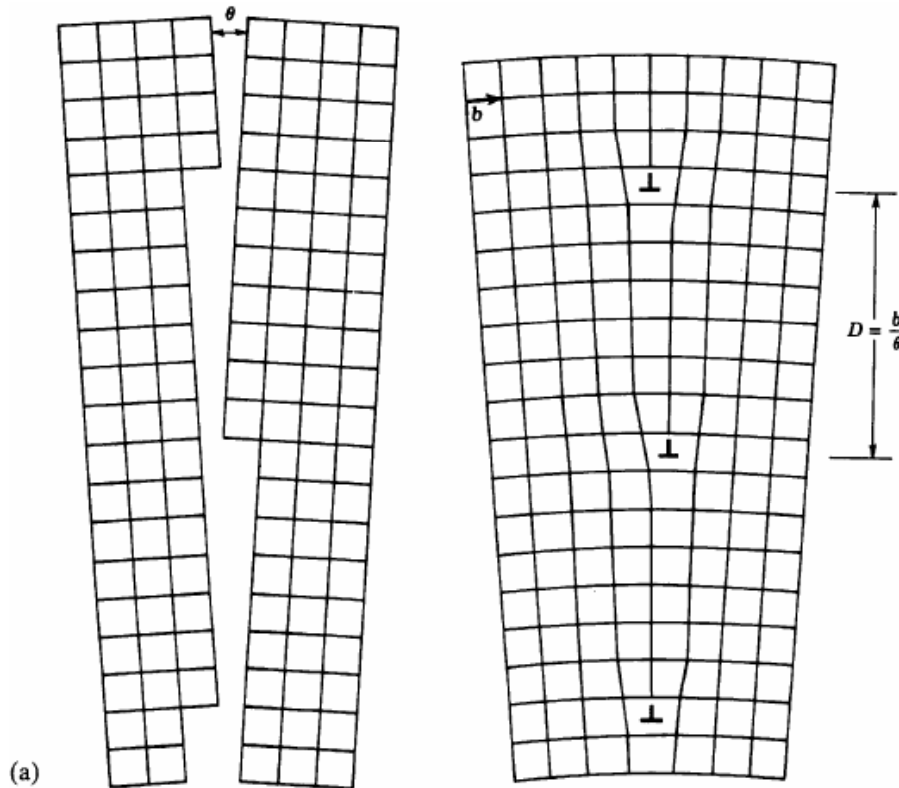
**In general boundaries of a mixture of the tilt and twist type,
→ several sets of different edges and screw dislocations.**

3.3.1 Low-Angle and High-Angle Boundaries

Low-Angle tilt Boundaries

→ around edge dislocation : strain ↑

but, LATB ~ almost perfect matching



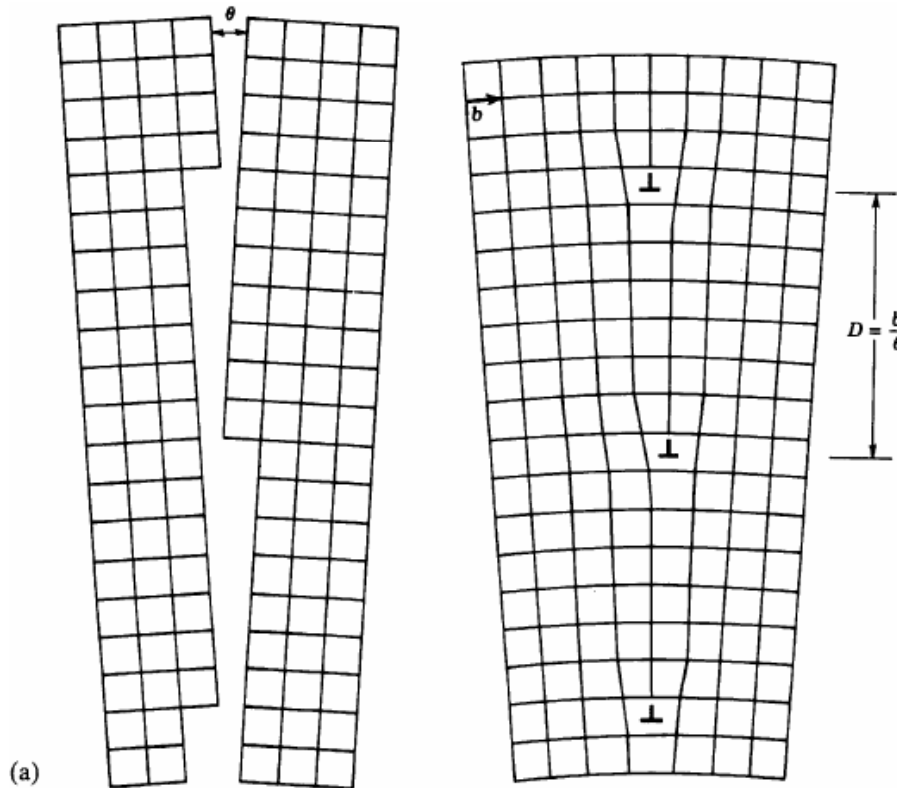
$$\sin \frac{\theta}{2} = \frac{b/2}{D}$$

$$\sin \frac{\theta}{2} \approx \frac{\theta}{2}$$

$$D \approx \frac{b}{\theta}$$

3.3.1 Low-Angle and High-Angle Boundaries

Low-Angle tilt Boundaries



→ around edge dislocation : strain ↑
but, LATB ~ almost perfect matching

→ g.b. energy : $\gamma_{g.b.}$ → E /unit area
(energy induced from dis.)

* Relation between D and γ ?

$\sin\theta = b/D$, at low angle

→ $D=b/\theta$ → $\gamma_{g.b.}$ is proportional to $1/D$

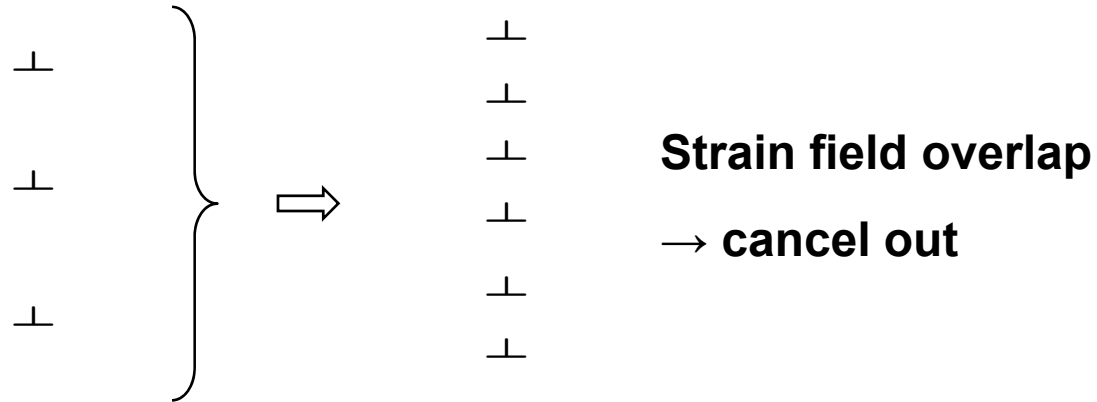
→ low angle tilt boundary

→ Density of edge dis.

(cf. low angle twist boundary → screw dis.)

Low-Angle tilt Boundaries

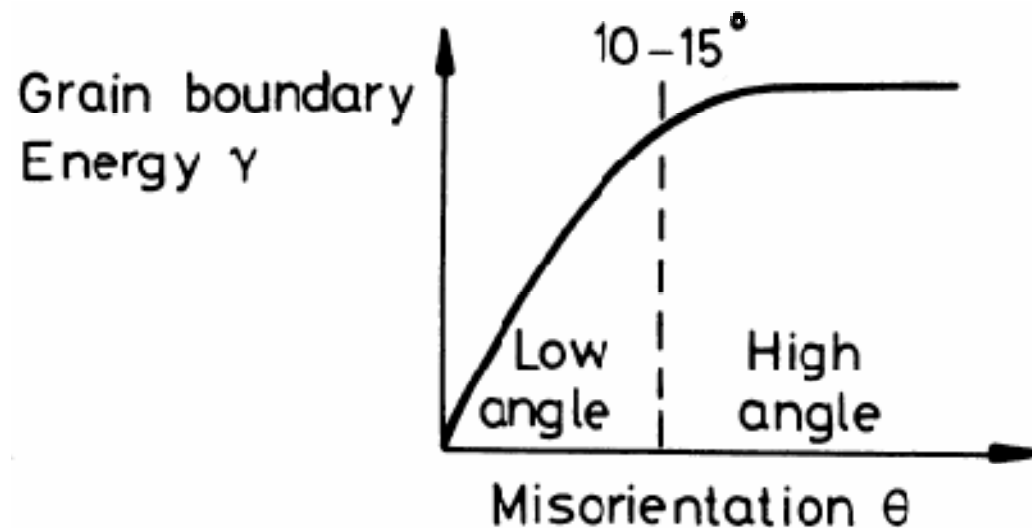
⇒ As θ increases, $\gamma_{g.b.} \uparrow$



→ $\gamma_{g.b.}$ increases and the increasing rate of γ ($=d\gamma/d\theta$) decreases.

→ if θ increases further, it is impossible to physically identify the individual dislocations

→ increasing rate of $\gamma_{g.b.} \sim 0$



Soap Bubble Model

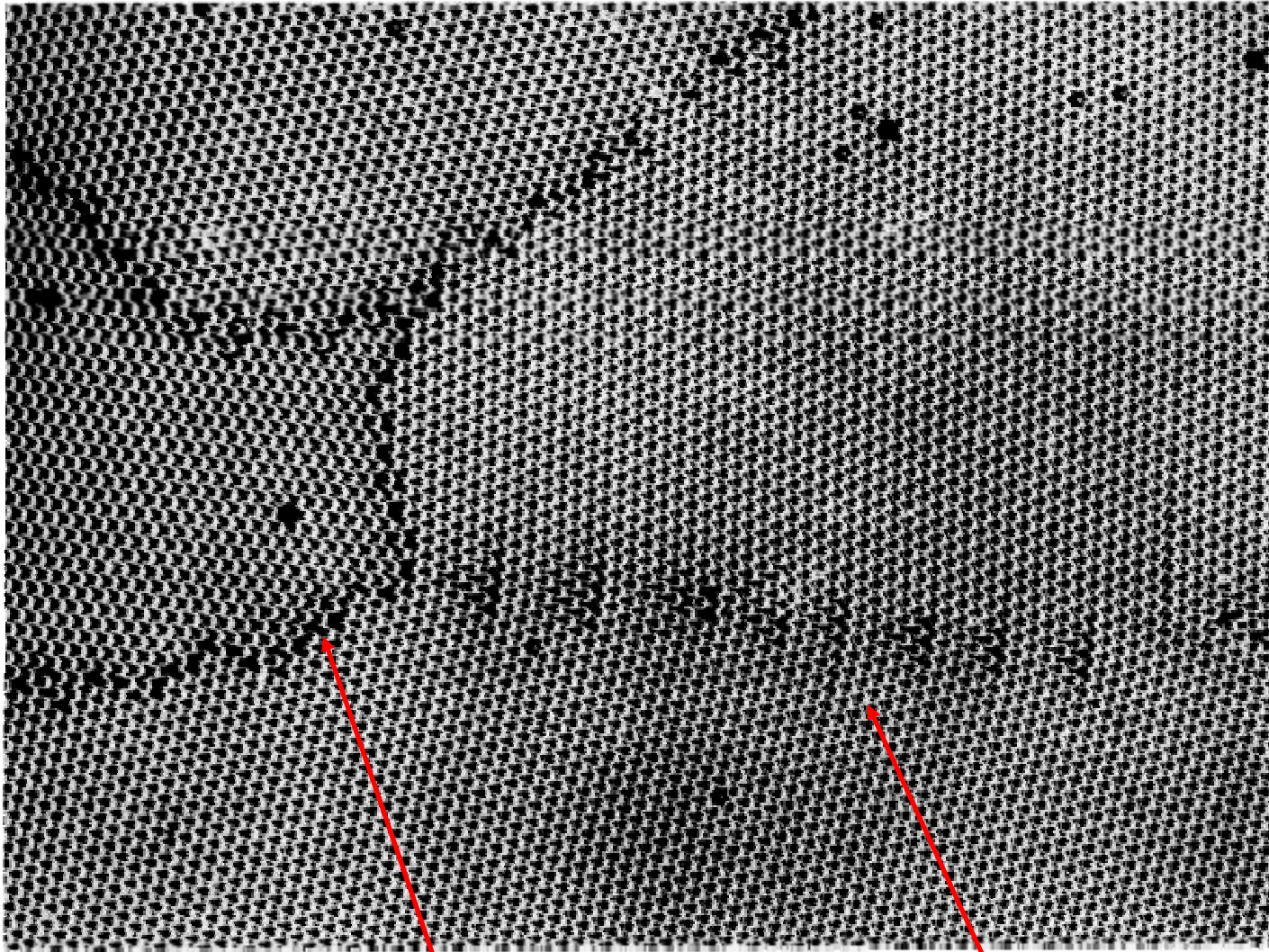


Fig. 3.11 Rafts of soap bubbles showing several grains of varying misorientation. Note that the boundary with the smallest misorientation is made up of a row of dislocations, whereas the high-angle boundaries have a disordered structure in which individual dislocations cannot be identified. (After P.G. Shewmon, *Transformations in Metals*, McGraw-Hill, New York, 1969, from C.S. Smith.)

High Angle Grain Boundary

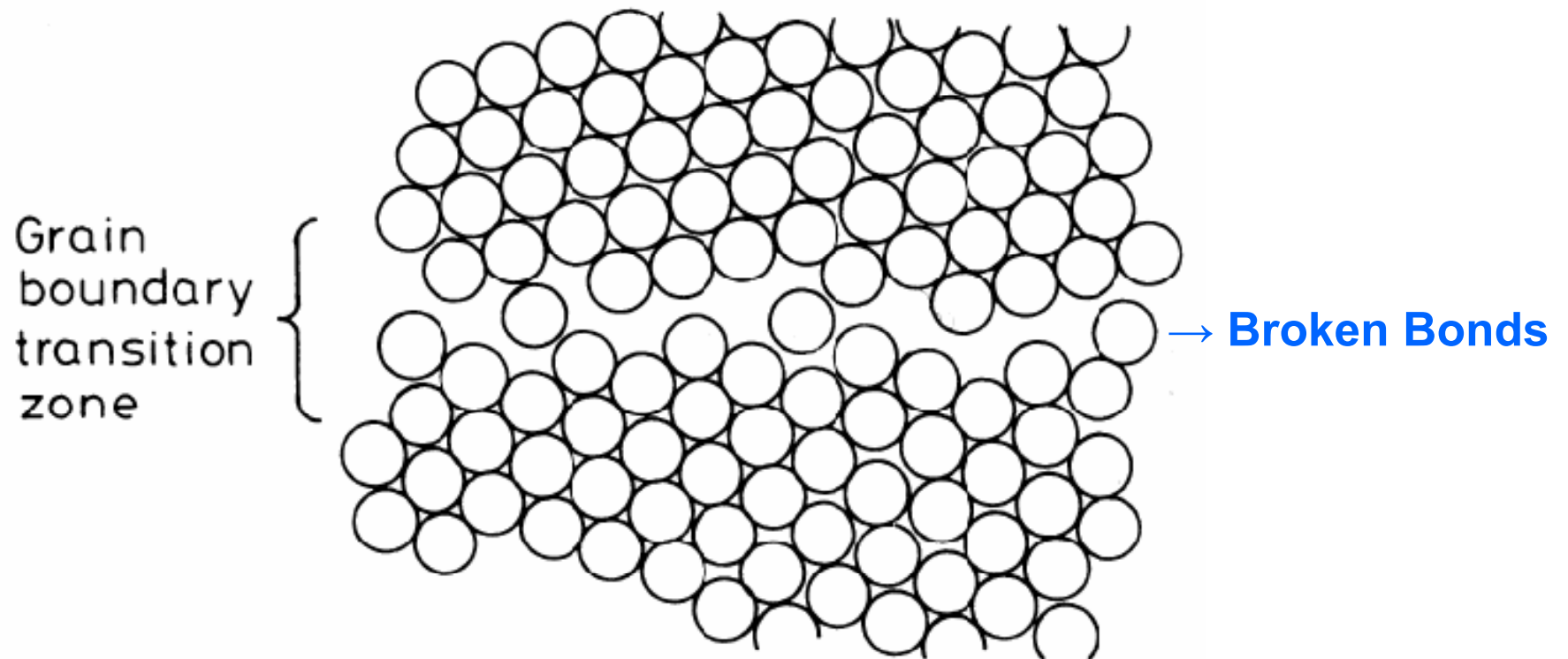


Fig. 3.10 Disordered grain boundary structure (schematic).

High angle boundaries contain large areas of poor fit and have a relatively open structure.

→ high energy, high diffusivity, high mobility (?) (cf. segregated gb)

High Angle Grain Boundary

- Low angle boundary
 - almost perfect matching (except dislocation part)
- High angle boundary (almost)
 - open structure, large free volume

* low and high angle boundary

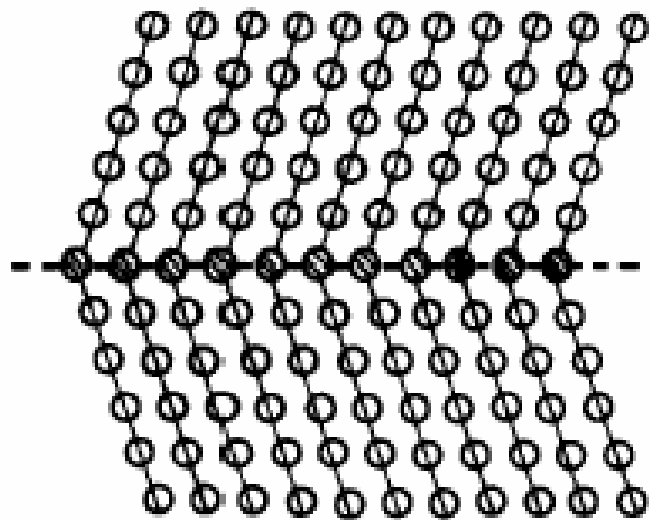
high angle $\gamma_{g.b.} \approx 1/3 \gamma_{sv}$ → Broken Bonds

Measured high-angle grain boundary energies

Crystal	$\gamma_b/\text{mJ m}^{-2}$	T/°C	γ_b/γ_{sv}
Sn	164	223	0.24
Al	324	450	0.30
Ag	375	950	0.33
Au	378	1000	0.27
Cu	625	925	0.36
γ -Fe	756	1350	0.40
δ -Fe	468	1450	0.23
Pt	660	1300	0.29
W	1080	2000	0.41

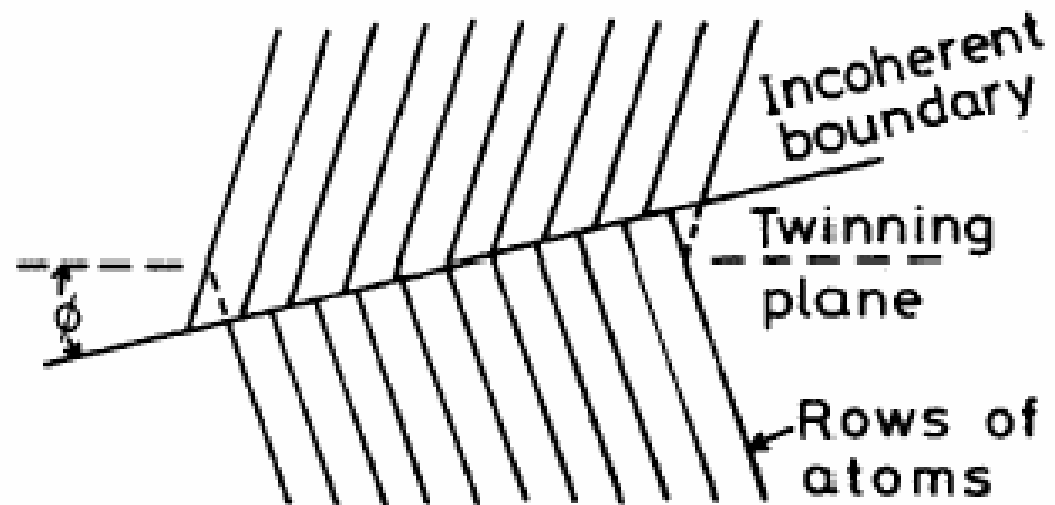
Special High-Angle Grain Boundaries

: high angle boundary but with low $\gamma_{g.b.}$



(a) **Coherent twin boundary**
symmetric twin boundary

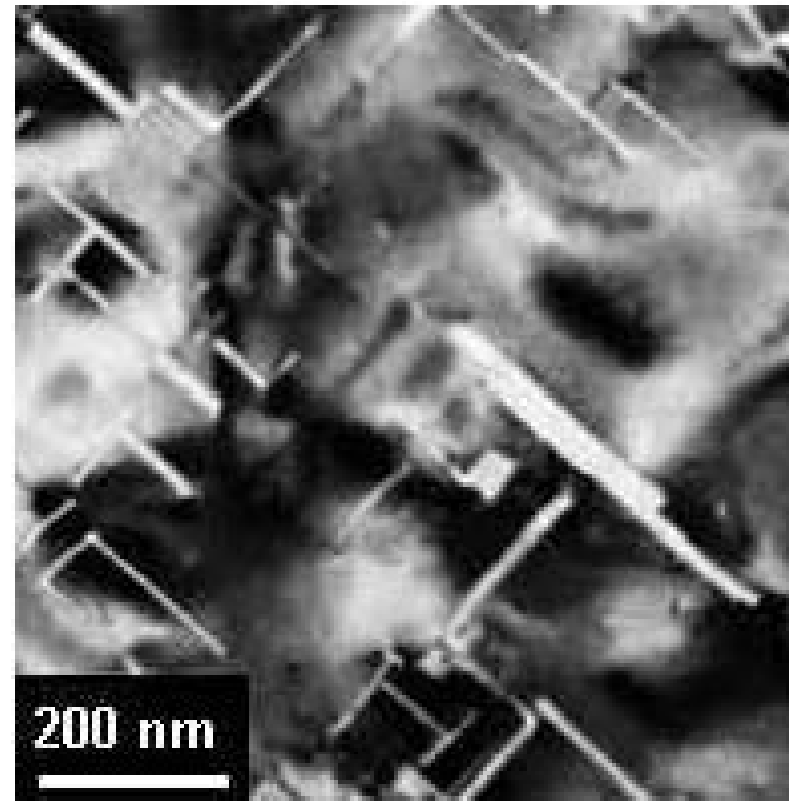
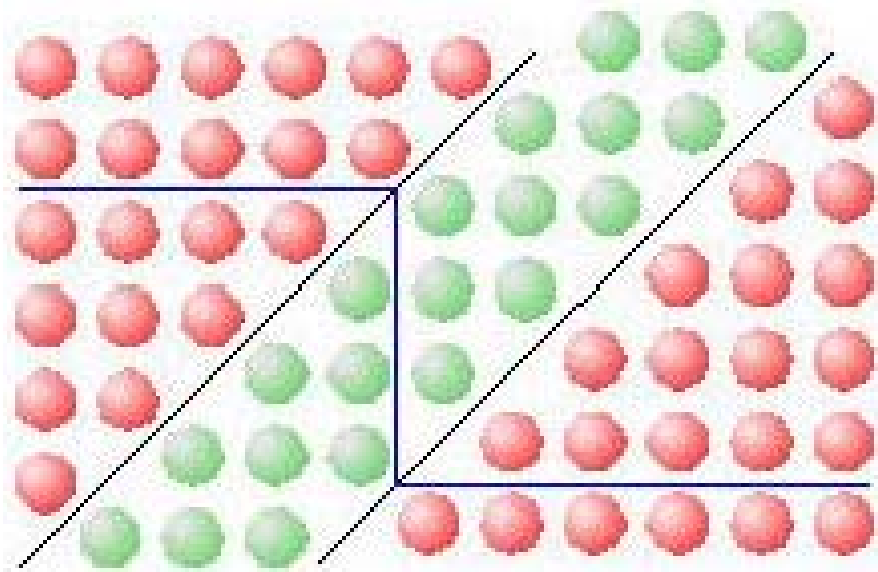
→ low $\gamma_{g.b.}$



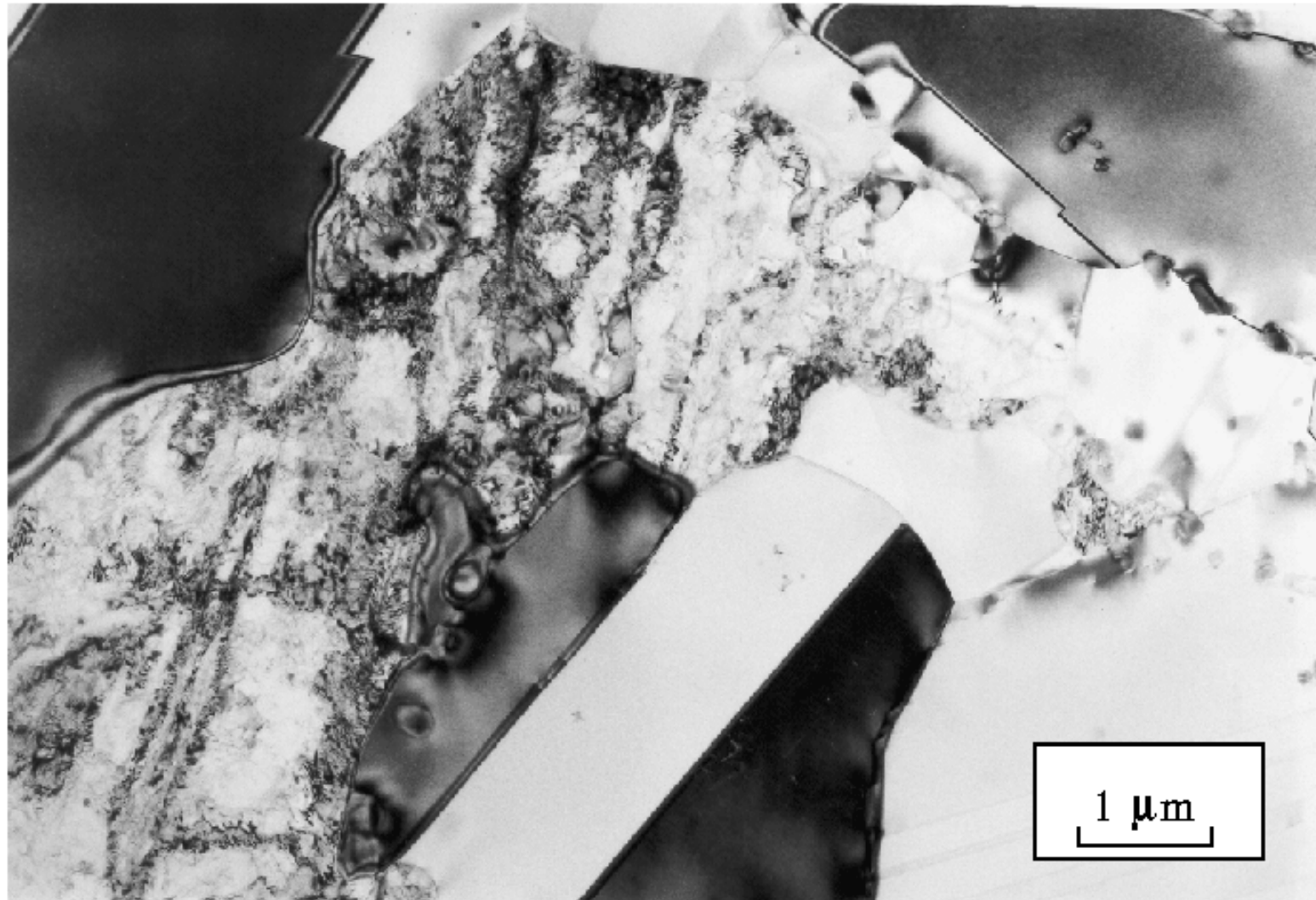
(b) **Incoherent twin boundary**
asymmetric twin boundary

→ low $\gamma_{g.b.}$

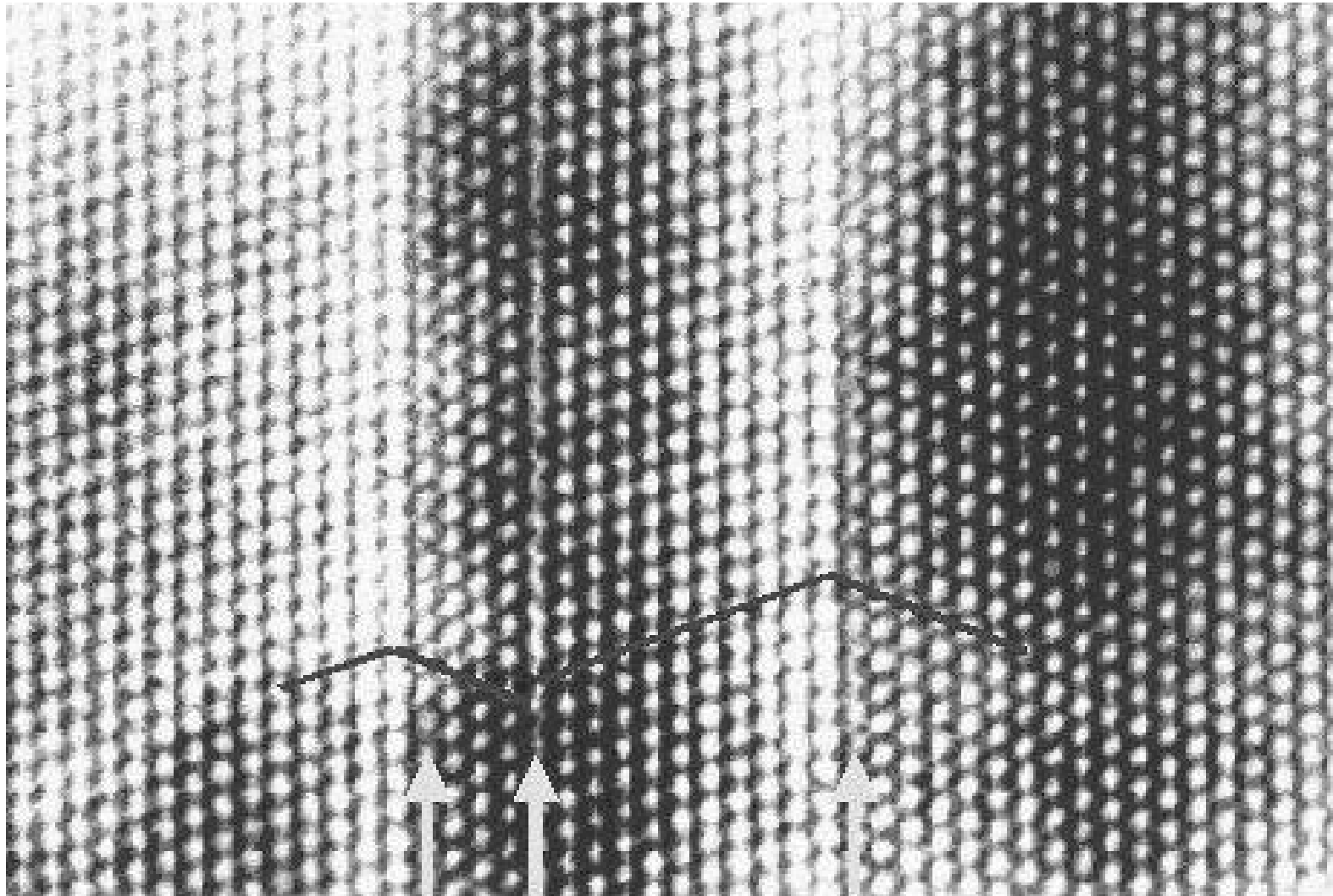
Twin boundary



Twin boundary



Twin boundary



Special High-Angle Grain Boundaries

(c) Twin boundary energy as a function of the grain boundary orientation

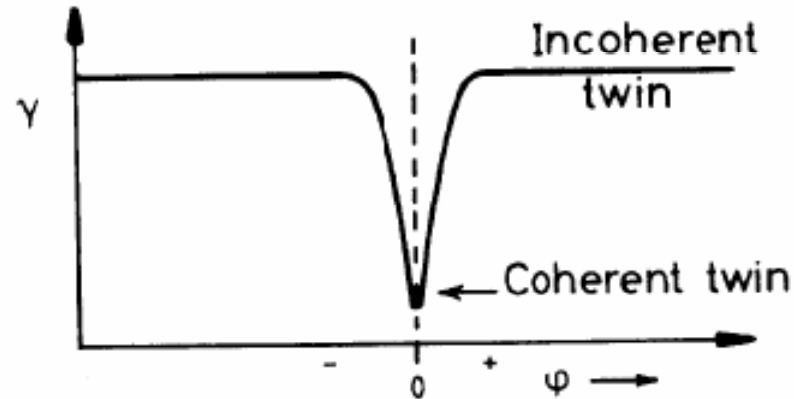


Table 3.3 Measured Boundary Free Energies for Crystals in Twin Relationships
(Units mJ/m^2)

Crystal	Coherent twin boundary energy	Incoherent twin boundary energy	Grain boundary energy
Cu	21	498	623
Ag	8	<< 126	< 377
Fe-Cr-Ni (stainless steel type 304)	19	209	835

Special High-Angle Grain Boundaries

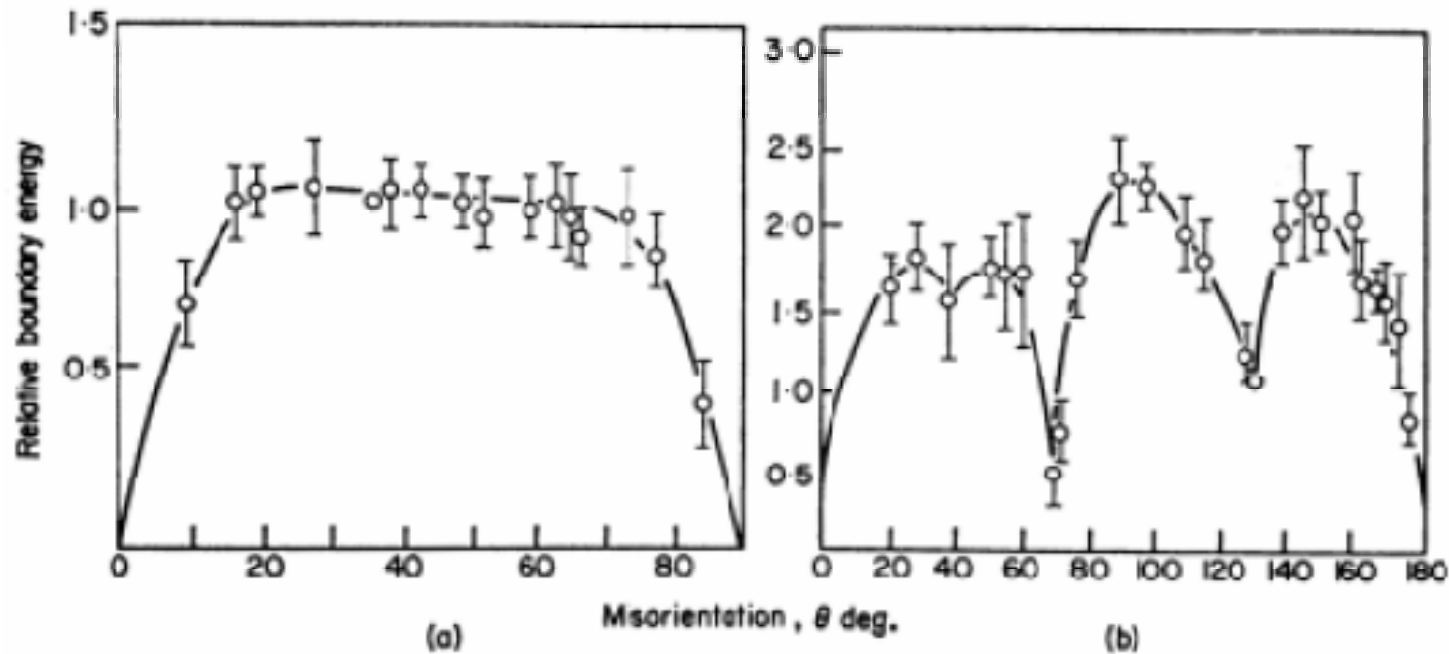


Fig. 3.13 Measured grain boundary energies for symmetric tilt boundaries in Al (a) When the rotation axis is parallel to $\langle 100 \rangle$, (b) when the rotation axis is parallel to $\langle 110 \rangle$. (After G. Hasson and C. Goux, Scripta Metallurgica, 5 (1971) 889.)

Why are there cusps in Fig. 3.13 (b)?

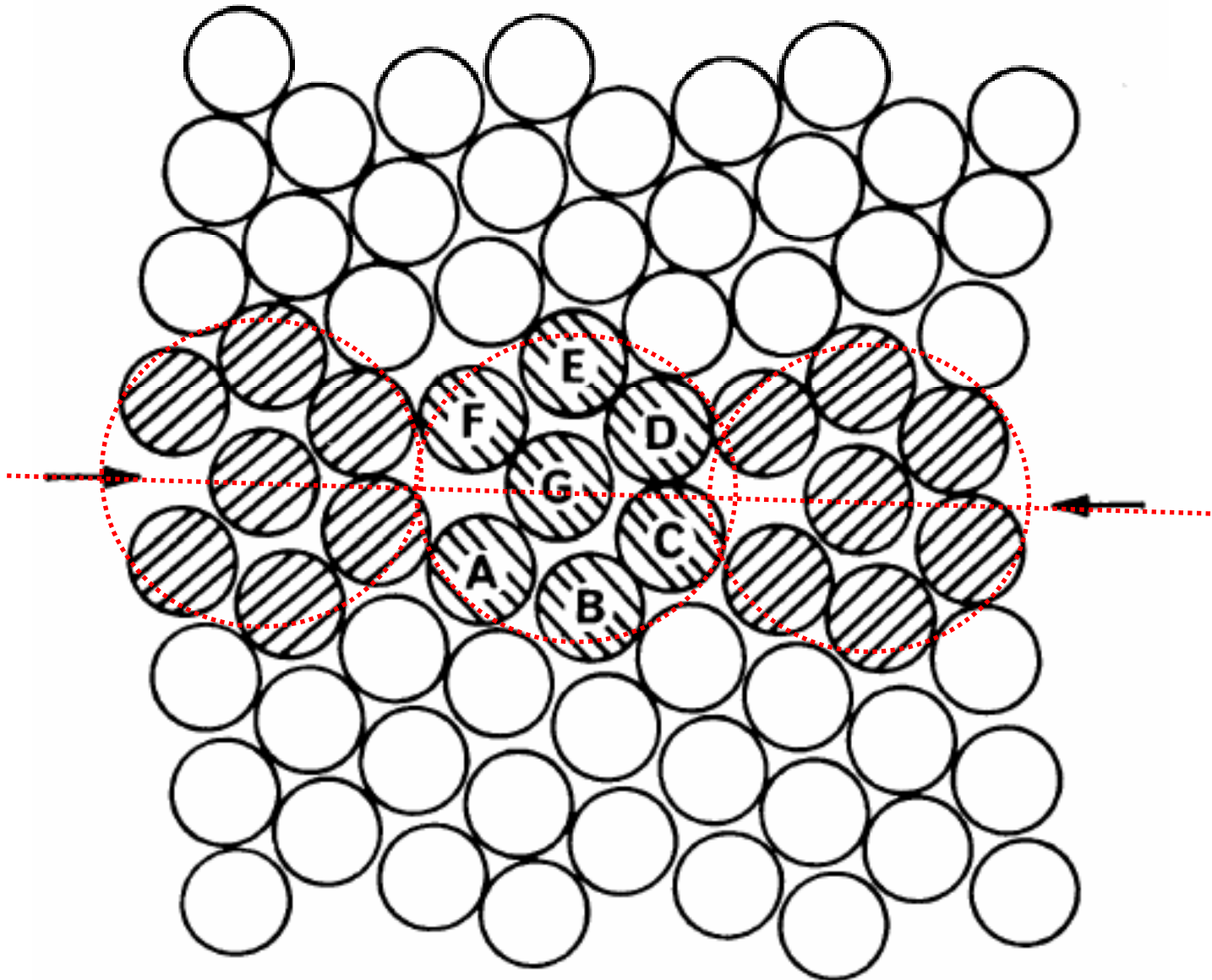


Fig. 3. 14 Special grain boundary. (After H. Gleiter, *Physica Status Solidi* (b) 45 (1971) 9.)

Equilibrium in Polycrystalline Materials

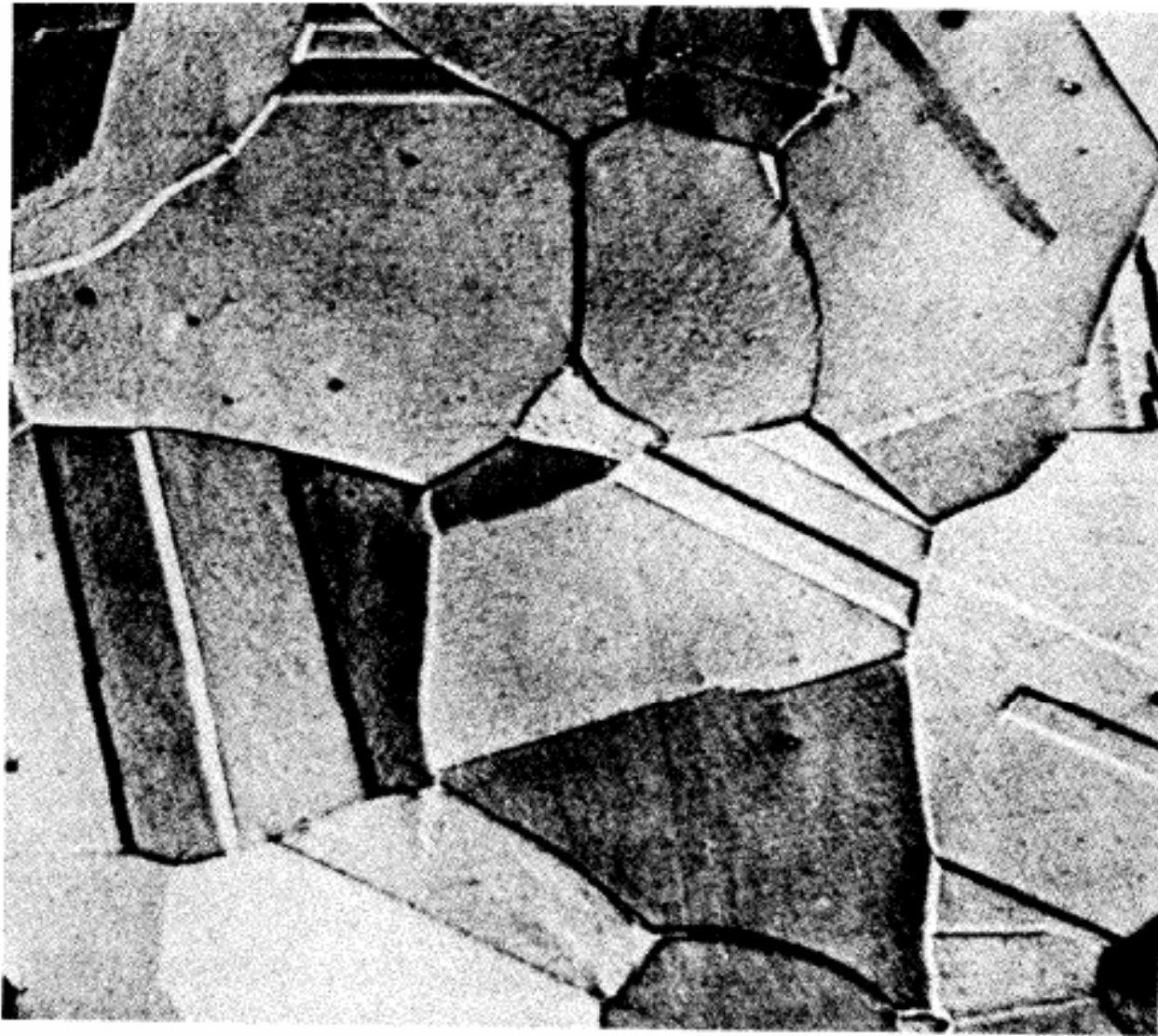


Fig. 3.15 Microstructure of an annealed crystal of austenitic stainless steel. (After P.G. Shewmon, *Transformations in Metals*, McGraw-Hill, New York, 1969)

Poly grain material

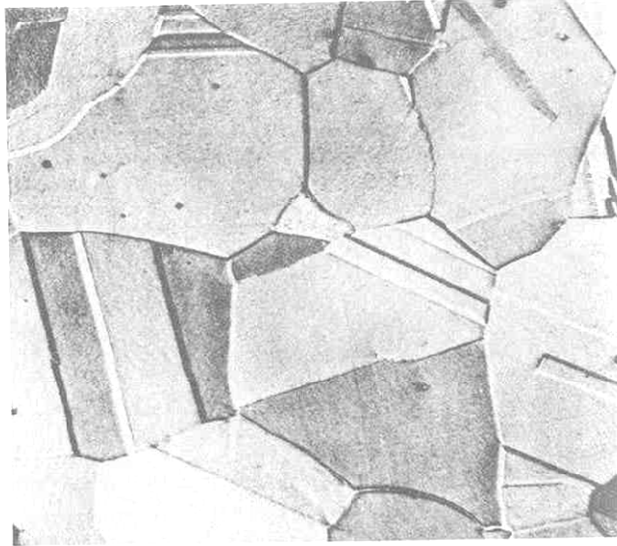
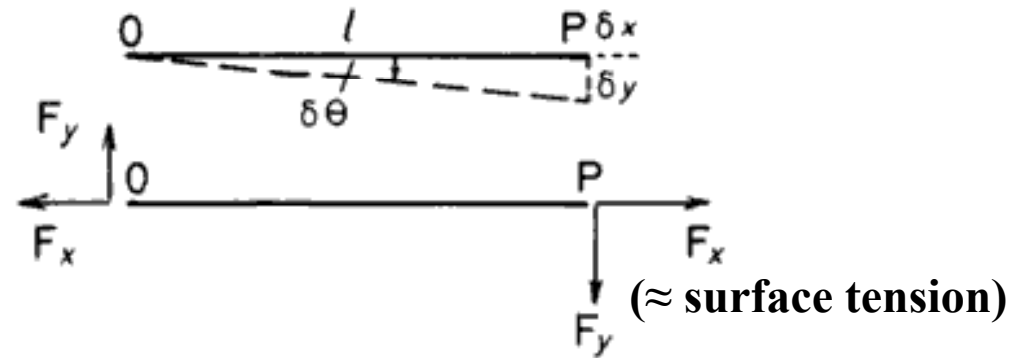


Fig. 3.15 Microstructure of an annealed crystal of austenitic stainless steel. (After P.G. Shewmon, *Transformations in Metals*, McGraw-Hill, New York, 1969.)

- $\gamma_{g.b.}$ → **metastable equilibrium**
(equil. (no g.b.))
- $\gamma_{g.b.}$ is minimum
- **force acting on junction of g.b. segment**



1) $F_x = \gamma$

2) $F_y ?$

P is moved at a small distance (δy)

A. work done by : $F_y \delta y$

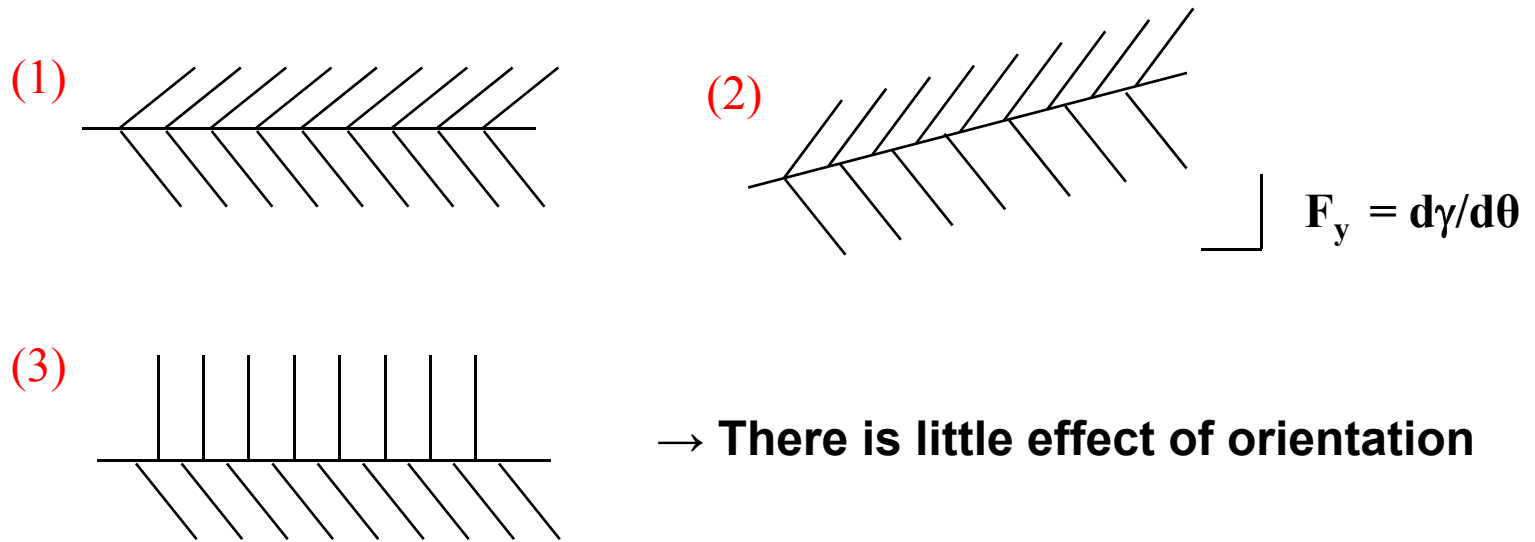
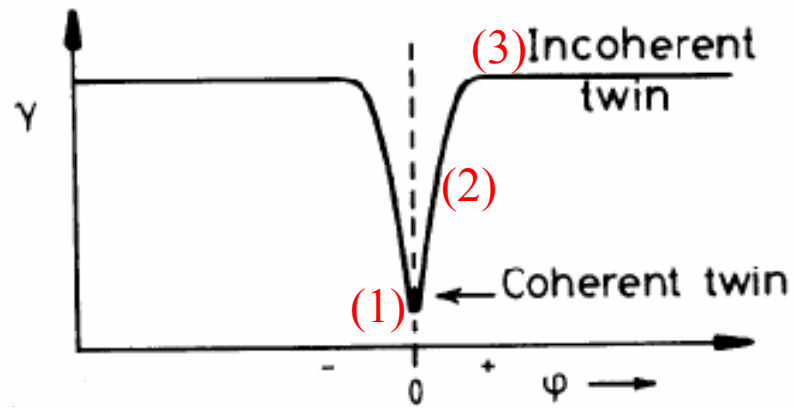
B. increase boundary energy caused

by the change in orientation $\delta\theta \sim l (d\gamma/d\theta) \delta\theta$

$$F_y \delta y = l (d\gamma/d\theta) \delta\theta$$

$$\rightarrow F_y = d\gamma/d\theta \quad \text{torque force}$$

→ **segment of g.b. moves to low energy position**

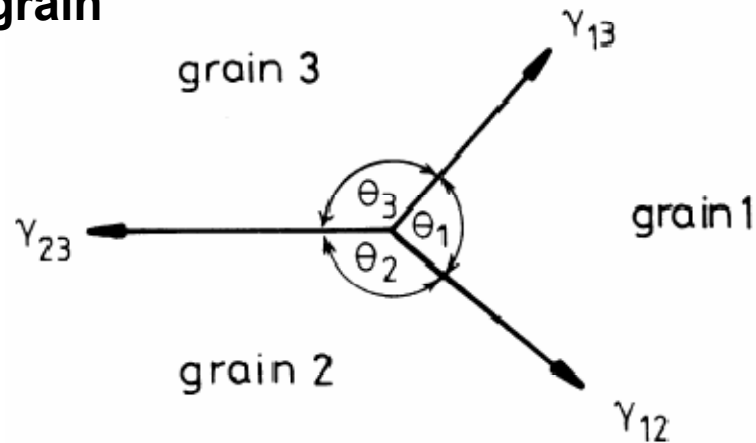


⇒ How metastable equil. ? → force (torque)

* general high angle boundary : $d\gamma/d\theta \approx 0$

→ consider more simply

→ 3 grain



$$\frac{\gamma_{23}}{\sin \theta_1} = \frac{\gamma_{31}}{\sin \theta_2} = \frac{\gamma_{12}}{\sin \theta_3}$$

→ $\theta = 120^\circ$

Measurement of grain-boundary energy using g.b groove profile
annealing a specimen at a high temperature and then measure the angle at the intersection of the surface with the boundary

If the solid-vapor energy (γ_{SV}) is the same for both grains,

$$2\gamma_{SV} \cos \frac{\theta}{2} = \gamma_b$$

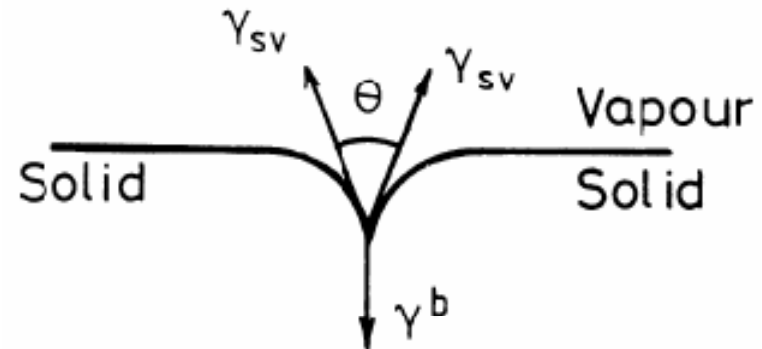


Fig. 3. 18 The balance of surface and grain boundary tensions at the intersection of a grain boundary with a free surface.

3.3.4. Thermally Activated Migration of Grain Boundaries

If the boundary is curved in the shape of cylinder, Fig. 3.20a, it is acted on by a force of magnitude γ/r towards its center of curvature.

Therefore, the only way the boundary tension forces can balance in three dimensions is if the boundary is planar ($r = \infty$) or if it is curved with equal radii in opposite directions, Fig. 3.20b and c.

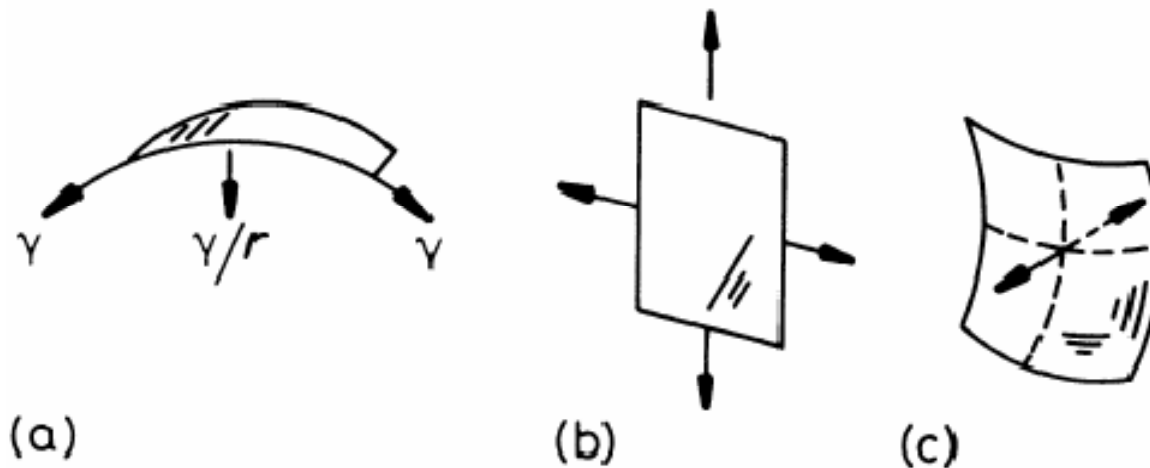


Fig. 3.20 (a) A cylindrical boundary with a radius of curvature r is acted on by a force γ/r . (b) A planar boundary with no net force. (c) A doubly curved boundary with no net force.

Direction of Grain Boundary Migration during Grain Growth

For isotropic grain boundary energy in two dimensions,
Equilibrium angle at each boundary junction? →120°

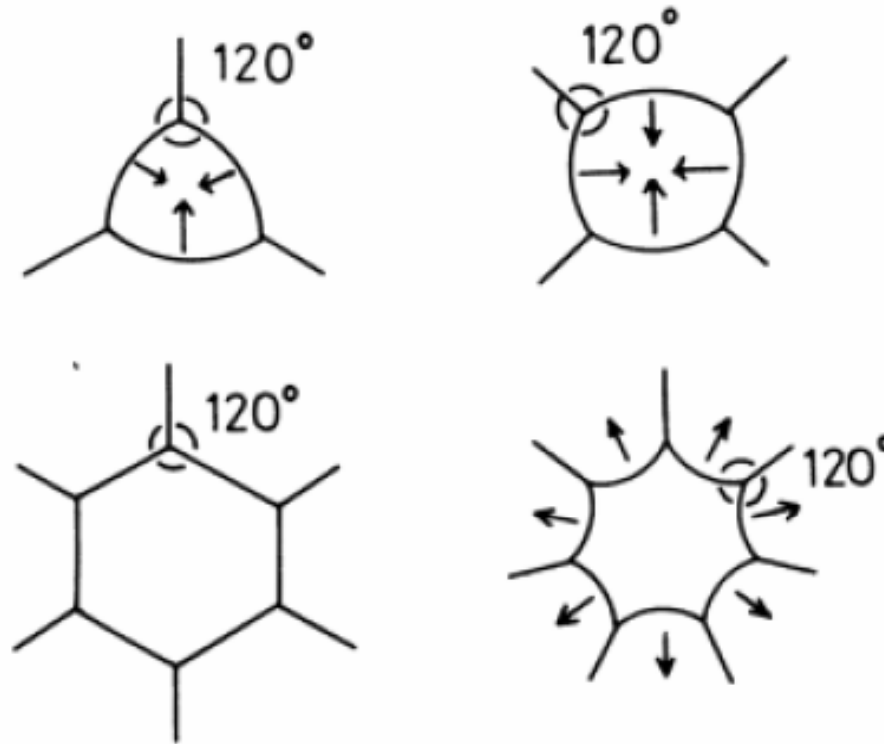


Fig. 3.21 Two-dimensional grain boundary configurations. The arrows in

Equilibrium angle at each boundary junction in 3D? →109°28'

Grain Growth (Soap Bubble Model)

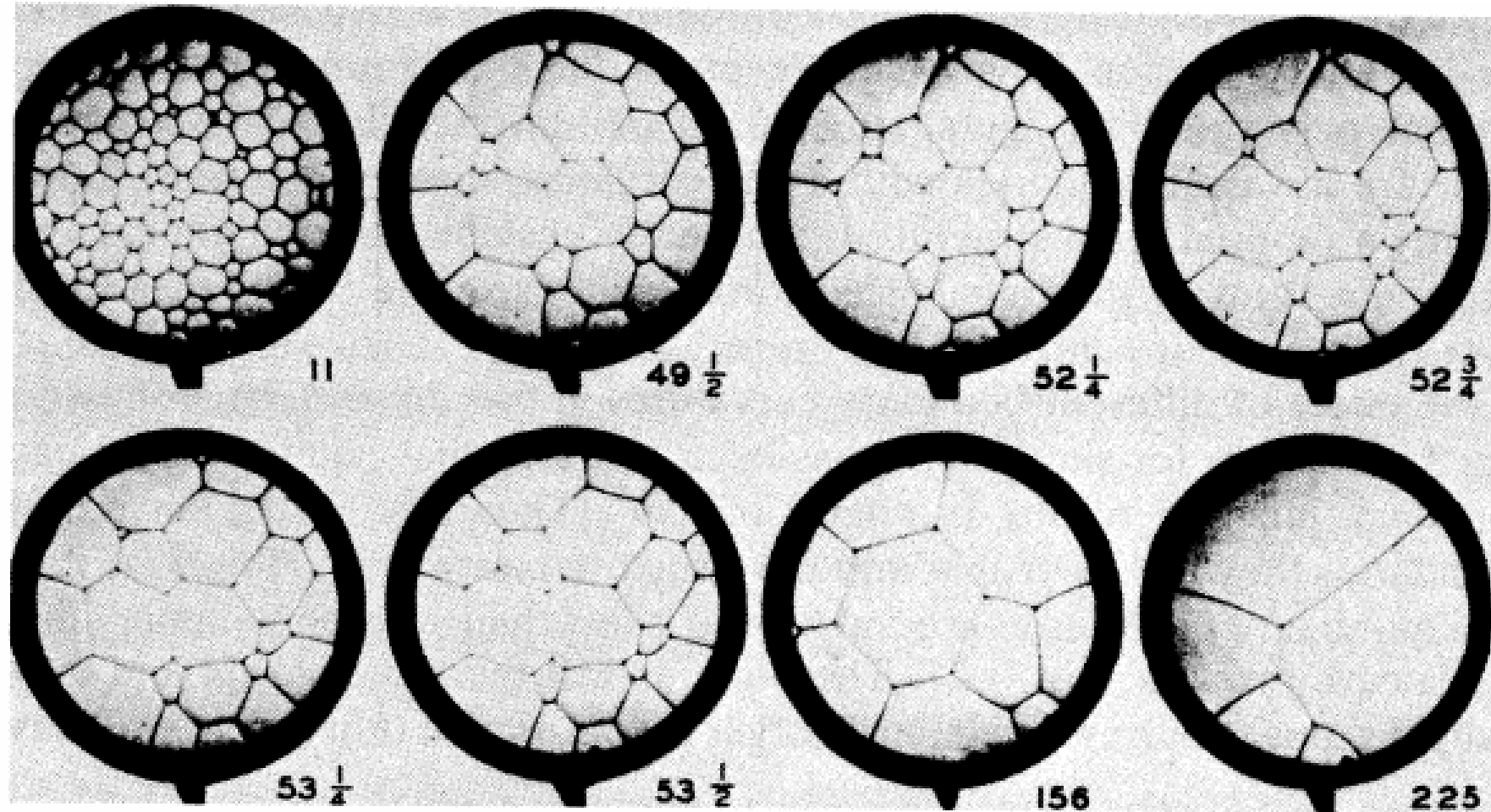
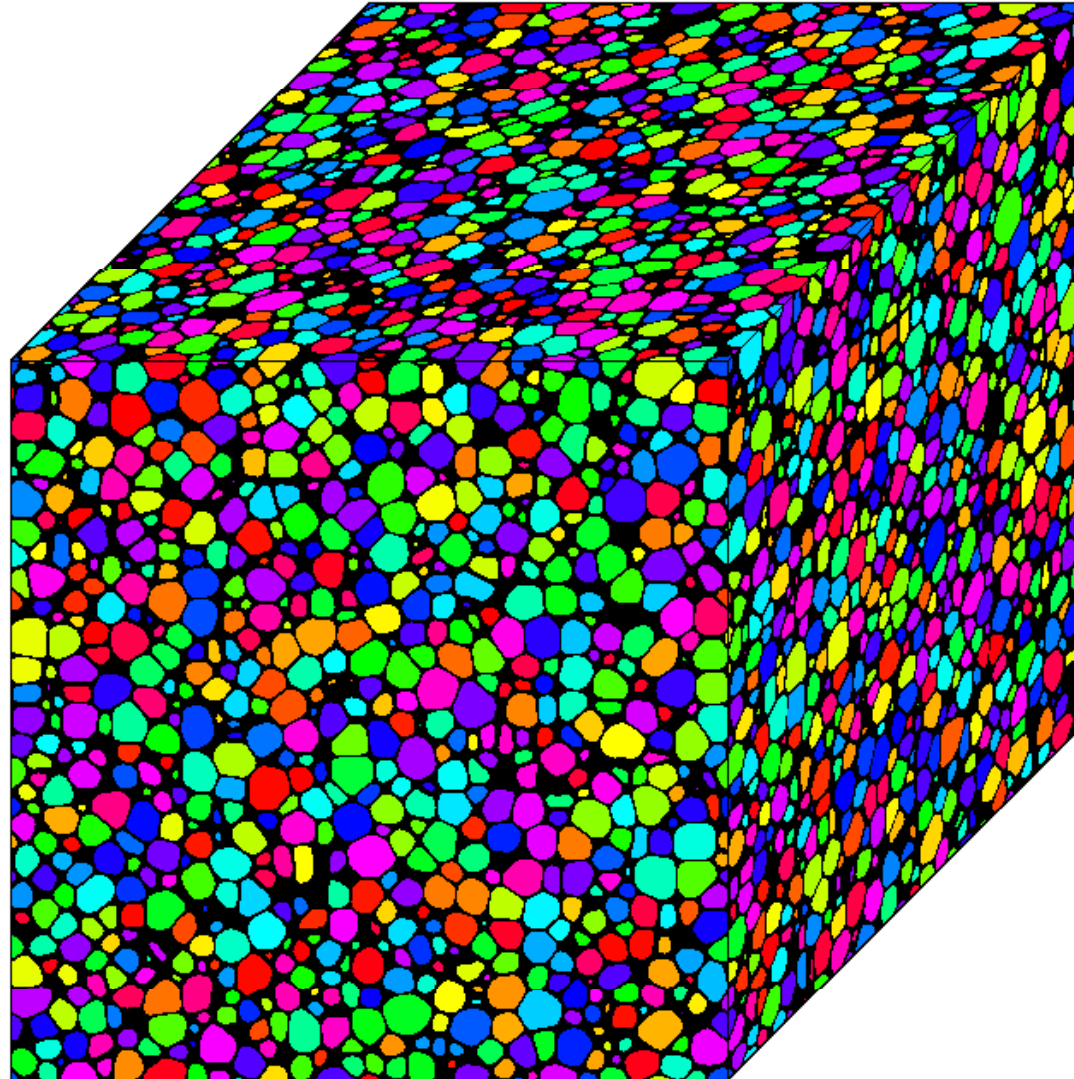


Fig. 3.22 Two-dimensional cells of a soap solution illustration the process of grain growth. Numbers are time in minutes. (After C.S. Smith, *Metal Interfaces*, American Society for Metals, 1952, p. 81.)

Example of Grain Growth simulation in 3D



A scenic autumn landscape featuring a valley filled with trees in various shades of green, yellow, and orange. In the background, there are rugged, rocky mountains under a clear blue sky. The foreground is partially framed by branches with vibrant red leaves on the right side.

결실의 계절 가을에
중간고사 준비 열심히 해서
모두 좋은 결과 있기를 ...^^